



Seventh Framework Programme FP7-SPACE-2010-1  
 Stimulating the development of downstream GMES services

Grant agreement for: Collaborative Project. Small- or medium scale focused research project

Project acronym: **SIDARUS**

Project title: **Sea Ice Downstream services for Arctic and Antarctic Users and Stakeholders**

Grant agreement no. 262922

Start date of project: 01.01.11

Duration: 36 months

Project coordinator: Nansen Environmental and Remote Sensing Center, Bergen, Norway

## D2.4: Submarine transect data from 2013

Due date of deliverable: 31.10.2013

Actual submission date: 23.01.2014

Organization name of lead contractor for this deliverable: UCAM

Project co-funded by the European Commission within the Seventh Framework Programme, Theme 6 SPACE		
Dissemination Level		
PU	Public	X
PP	Restricted to other programme participants (including the Commission)	
RE	Restricted to a group specified by the consortium (including the Commission)	
CO	Confidential, only for members of the consortium (including the Commission)	

ISSUE	DATE	CHANGE RECORDS	AUTHOR
1	23/01/2014	Version 1	R. Clancy

### **SIDARUS CONSORTIUM**

Participant no.	Participant organisation name	Short name	Country
1 (Coordinator)	Nansen Environmental and Remote Sensing Center	NERSC	NO
2	Alfred-Wegener-Institut für Polar-und Meeresforschung	AWI	DE
3	Collecte Localisation Satellites SA	CLS	FR
4	University of Bremen, Institute of Environmental Physics	UB	DE
5	The Chancellor, Masters and Scholars of the University of Cambridge	UCAM	UK
6	Norwegian Meteorological Institute, Norwegian Ice Service	Met.no	NO
7	Scientific foundation Nansen International Environmental and Remote Sensing Centre	NIERSC	RU
8	B.I. Stepanov Institute of Physics of the National Academy of Sciences of Belarus	IPNASB	BR

No part of this work may be reproduced or used in any form or by any means (graphic, electronic, or mechanical including photocopying, recording, taping, or information storage and retrieval systems) without the written permission of the copyright owner(s) in accordance with the terms of the SIDARUS Consortium Agreement (EC Grant Agreement 262922).

All rights reserved.

This document may change without notice

## Table of Contents

<b>CHAPTER 1: INTRODUCTION</b> .....	<b>3</b>
<b>CHAPTER 2: SUMMARIES</b> .....	<b>4</b>
2.1 AS11 .....	4
2.2 AS12 .....	6
<b>CHAPTER 3: MEASUREMENTS/RESULTS</b> .....	<b>8</b>
3.1 AUV DATA .....	8
3.2 LiDAR .....	14
3.3 DRILL LINES .....	19
3.4 AERIAL IMAGING .....	21
<b>CHAPTER 4: DISCUSSION</b> .....	<b>23</b>
4.1 AUV .....	23
4.2 LiDAR .....	24
4.3 DRILL DATA.....	25
<b>CHAPTER 5: APPENDIX: AS11 DRILL LINE PROFILES</b> .....	<b>27</b>

## *List of Figures*

Figure 1.....	6
Figure 2.....	8
Figure 3.....	10
Figure 4.....	11
Figure 5.....	11
Figure 6.....	12
Figure 7.....	13
Figure 8.....	14
Figure 9.....	15
Figure 10.....	16
Figure 11.....	17
Figure 12.....	18
Figure 13.....	19
Figure 14.....	20

Figure 15.....	20
Figure 16.....	21
Figure 17.....	22
Figure 18.....	22
Figure 19.....	23
Figure 20.....	24
Figure 21.....	26

### ***List of Tables***

Table 1.....	6
Table 2.....	8

### ***SUMMARY***

We report on field experiments and results achieved during experiments in Fram Strait from R.V. "Arctic Sunrise" carried out in the summers of 2011 and 2012. The 2011 experiments involved high-resolution mapping of the upper ice surface using a laser scanning system supplied by Scan Lab Ltd. These experiments were repeated in 2012 but with the addition of an AUV (autonomous underwater vehicle) rented from Woods Hole Oceanographic Institution, and equipped with a Geoswath multibeam sonar to record the three-dimensional structure of the ice underside. The collocation of the high-resolution measurements of the ice upper and lower side in selected pressure ridges permits not only an unprecedented quality of measurement of pressure ridge morphology but also a large number of accurate freeboard-draft correlations which are important for validation of satellite borne ice thickness measuring systems such as the CryoSat-2 radar altimeter. One of the ridges sampled in this way was a type of ridge never before mapped quantitatively, a *stamukha*, or large, thick (28 m draft) isolated ridge which has spent a number of summers aground on the Siberian shelf before melting enough to drift off the seabed and join the moving pack. It could be identified by its exceptionally low salinity and covering of dirt, from Siberian river overflows.

## Chapter 1: Introduction

New record minima of sea ice are being reported year after year. The data behind these results stems almost exclusively from satellite mounted radars. Modern satellite technology is very accurate in measuring the surface area covered by sea ice, but still struggles to reliably measure the thickness of the highly variable ice cap. Up to now, satellite measurements appear to be biased in that they get more returns from bigger floes. The relation between floe size and thickness in the MIZ is thus of crucial interest, as one example. The data set collected during this project (with its large number of floes) will provide an excellent opportunity to study this relation, amongst others.

As the Arctic ice retreats further, the traditional idea of the Arctic sea ice as being strongly confined by surrounding landmass begins to lose justification. Over the coming years the ice pack will be increasingly subjected to divergent wind and current stresses, which will lead to a thinner and more loosely packed ice regime - resembling the seasonal sea ice cover of the Southern Ocean. In order to get a complete characterization of the ice, comparison of high resolution surface topography data and corresponding underside scans are called for. To achieve this we tested the surface LiDAR scanning equipment during a trial cruise in 2011 and added AUV-mounted multibeam sonar during a follow-up expedition in 2012. This means not only a more complete survey but also a temporal continuity that will help understand the evolution of the ice over time. The BAS ICEBELL cruise (2010) to the Weddell and Bellingshausen Seas collected a similar data set, as well as the SIPEX-II cruise in September- November 2012 to the East Antarctic. Not only being of great scientific value in their own right, comparing these data sets will be a first step in finding out whether the Arctic is approaching the conditions of the Antarctic.

## Chapter 2: Summaries

### 2.1 AS11

In September 2011, the authors led a research expedition (henceforth: AS11) to Fram Strait aboard “Arctic Sunrise” to monitor sea ice conditions. Our purpose was twofold: a) help validate and calibrate satellite measurements in the marginal ice zone (MIZ) and b) gather high resolution data of deformed sea ice that will provide new insights into the physical processes underlying sea ice mechanics and dynamics. This was mainly designed to be a test-run for a more comprehensive cruise (see next section). In order to achieve these goals we performed a variety of observations, including ice core sampling, snow depth measurements, thickness readings, aerial imagery and 3D laser scanning. A total of 17 ice floes were surveyed. The final data set includes 77 panoramic 3D laser scans, over 350 ice thickness measurements and several thousand aerial images.

Three sets of observations were conducted, with 3-10 floes at each site. The first period of observations took place between Sept 4-11 at  $80^{\circ}40' - 80^{\circ}50'N/1^{\circ}15'E-1^{\circ}25'E$ . Three floes were measured on this leg of the experiment. Detailed scans, representative drill-lines (10-20 holes) and corresponding snow depths were collected, as well as ice-core samples for floes 1 and 2. After a brief return to Longyearbyen, Svalbard, to exchange personnel, the second leg of the experiment took place from Sept 15-18 around  $79^{\circ}15'-35'N/2^{\circ}E-3^{\circ}28'W$ . On floes 4 and 6 a large number of scans was performed (12 and 24, respectively), together with extensive drilling lines (41 holes/4 lines, 51 holes/5 lines, respectively) to give detailed topographies of the floes at hand. On Sept 16, a small crew of 3 scientists measured five small floes (5A-E) in the vicinity of the ship to obtain a representative picture of the ice conditions in this region of the marginal ice zone. The scientists were dropped on the (pseudo-)randomly chosen floes by helicopter to collect a single scan and a drill line (5-8 holes) on each floe. On Sept 17, two scientists and one crew member flew North, stopping at intervals of ca. 10 nm, to measure the evolution of ice thickness from the ice edge northwards. Drill lines were obtained on four different floes (7A-D), with approximately 10 holes each, apart from floe 7D, a MY floe, which featured average thicknesses of  $\sim 4m$ , so that after 4 holes the crew returned to the ship due to time constraints. After another stopover in Longyearbyen, the third leg of the cruise took place on Sept 21/22 close to the location of the second (at  $79^{\circ}8'-11'N/0^{\circ}20'W-4^{\circ}27'W$ ). Due to foggy conditions with little visibility and repeated sightings of polar bears in the vicinity of the ship, the time spent collecting data was limited on this last leg. However, a total of 103 drill holes (6 lines) and 3 scans could be obtained on floe 9, as well as 3 high resolution scans and a 12-hole drill line on floe 10. In general throughout this cruise, the floes measured were chosen to give a representative picture of the of the local ice conditions - with exception of floes 3 and 6 which were selected for their intricate topographies.

The collected data are presented and discussed in section 3.

Date	Floe	Lat/Lon	Scanner	Drill Data	Imagery	Survey Data	Snowdepths	Cores
03/09	1	80°42.9' N, 2°25.5' E	8	23 (ALine)	✓	27 (random)	30 (ALine)	1
04/09 05/09	2 <sup>a</sup>	80°43.1' N, 2°17.0' E	11	12 (ALine) 11 (BLine) 12 (CLine)	✓	78 (ALine+) <sup>b</sup> 108 (BLine+Peri)	31 (ALine) 61 (   ALine) 114 (→Survey)	2
09/09 - 11/09	3 <sup>c</sup>	80°52.1' N, 1°27.7' E	6	22 (ALine)	-	279 (ALine+Peri) <sup>d</sup> 1012 (Grid)	16 (ALine) 14 (random)	-
15/09	4	79°38.3' N, 2°02.6' E	12	11 (ALine) 11 (BLine) 8 (CLine) 11 (DLine)	✓	-	no signif. snow	1
16/09	5A 5B 5C 5D 5E	79°26.4' N 2°31.8' W	2 1 1 1 2	8 (5m int.) 6 ( " ) 6 ( " ) 5 ( " ) 5 ( " )	✓	-	-	-
17/09 18/09	6	79°16.5' N, 3°28.3' W	24	11 (ALine) 22 (BLine) 18 (CLine)	✓	-	no signif. snow	3
17/09	7A <sup>e</sup> 7B 7C 7D	79°23.9' N, 3°47.3' W 79°32.5' N, 4°08.0' W 79°43.4' N, 4°18.2' W 79°55.4' N, 4°17.5' W	-	10 (5m int.) 11 ( " ) 10 ( " ) 4 ( " )	✓	-	-	-
18/09	8	79°06.3' N, 3°42.8' W	3	9 (5m int.)	-	-	no signif. snow	1
21/09	9	79°8.2' N, 0°20.4' W	3	103 (6 Lines)	✓	110 (6 Lines)	110 (6 Lines)	1
22/09	10	79°11.4' N, 4°27.4' W	3 (hi-res)	12 (ALine)	-	16 (ALine)	16 (ALine)	-

Table 1: Overview of measurements taken during the AS11

<sup>a</sup>Floe 2 broke up into 2 pieces halfway through drilling the ALine

<sup>b</sup>Consists of 2 data files: FL\_2\_5\_9\_11.txt and FL2UNDEF2.txt

<sup>c</sup>Floe 3 broke up into 2 pieces after the 9th

<sup>d</sup>First set of survey points taken 09/09, second set taken 10/09 after break up

<sup>e</sup>Floes 7 were measured every 10nm going north from the ship (Floe6)

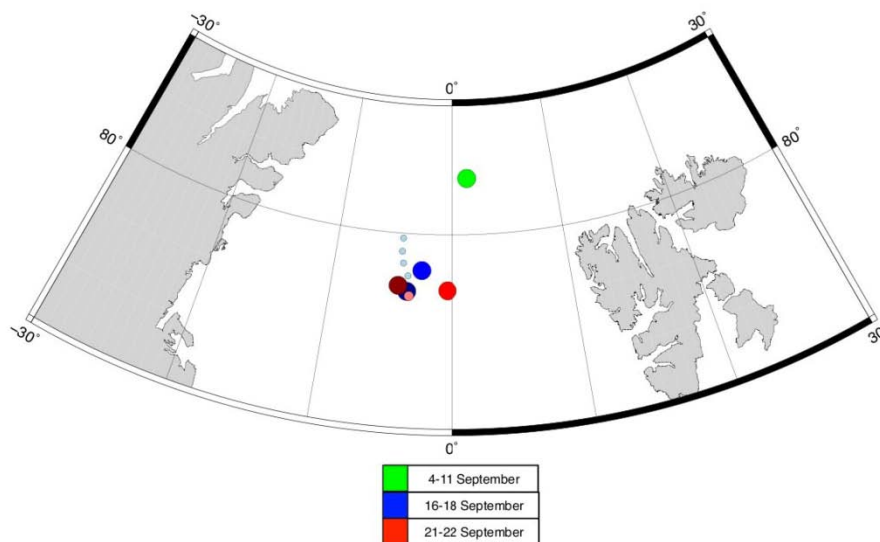


Figure 1: Map of locations visited during field experiment AS11.

## 2.2 AS12

A second field operation, this time to measure simultaneously the surface and underside topography of pressure ridges, was carried out between July 9 and 21 2012, again using MV "Arctic Sunrise" by courtesy of Greenpeace. DAMTP personnel were Prof Peter Wadhams (chief scientist), postdoc John Fletcher and graduate students Till Wagner and Nick Toberg. The underside was profiled by a Sea Bed AUV of Woods Hole Oceanographic Institution, which was operated by Dr Hanu Singh and two assistants. The surface topography was obtained in high resolution by Laser Scan (William Trussell).

The ship started from Longyearbyen, where the AUV was calibrated and tested, on July 10, and sailed to meet the ice edge in Fram Strait at a location (79° 32'N, 0° 40'E) corresponding to a Radarsat quadpol retrieval expected on July 14 and ordered by the Norwegian Meteorological Institute (Nick Hughes) as part of their participation in Sidarus. The ship was in 50% concentration first-year (FY) and multi-year (MY) floes when it reached this position.

The first floe selected, floe 1, was a large, long MY floe carrying a classic triangular ridge, a low rolling hummock and a lot of rubble. The ship was moored to the floe, the Laser Scan operation carried out as well as several cores drilled, and several lines of thickness holes drilled, in order to obtain optimal co-registration between laser and AUV.

Floe 2, in the same vicinity, was a **stamukha**, a very old isolated pressure ridge, covered in dirt and of considerable draft (28 m), which is a feature of the shelf seas north of Siberia. They are ridges which run aground and remain fast to the seabed through a summer when all the ice around them melts, leaving the stamukha as a grounded isolated island. It may remain for a number of years at a given site (typically a coastal site on the Siberian shelf) before lifting off through melt and joining the Arctic circulation, to emerge through Fram Strait as a real rarity. To our knowledge no stamukha has been studied before in this intense way, and once again we were able to obtain AUV multibeam mosaics of the underside and laser scans of the topside.

Floe 3, on July 16, had a well developed ridge complex on one edge of a very large (2 km) floe. The first AUV transit was successful, but a second mosaic resulted in the vehicle being carried into the centre of the floe through not having sufficient power to stem a strong relative current moving under the floe. The AUV was lost and could not be recovered despite a day of searching; it was insured by WHOI.

Floe 4 was mapped only on the upper surface by the laser, with drilled and cored holes. It was overflowed at low level by the Basler Polar 5 aircraft of Alfred Wegener Institute on July 18, equipped with an EM-31 electromagnetic ice thickness profiling system.

Finally, floe 5 was profiled by laser and found to be a thick FY floe with well-defined linear ridges. This was the floe which was profiled by the AWI aircraft.

All floes had lines of holes drilled across them to provide a tie-in between the surface and bottom topographies recorded by the two types of instrument. Floe locations were chosen so as to be within the range of successive Radarsat quadpol retrievals, to be monitored and analysed by Nick Hughes at Norwegian Meteorological Institute.

Table 2: Overview of the measurements taken during AS12:

Date	Floe	Lat/Lon	AUV	#Scans	#Drill Data	#Snow Data
14/07	2 <sup>†</sup>	79° 43.019' N, 0° 26.704' E	Yes	11	-	N/A
15/07	3	79° 48.125' N, 0° 12.442' E	Yes <sup>*</sup>	9	41	41
16/07	4	79° 50.081' N, 0° 29.350' E	Yes <sup>‡</sup>	11	12	9
19/07	5	79° 30.016' N, 0° 02.785' W	No	8	13× 4(lines)	13× 4(lines)

<sup>†</sup> Stammkha - the floe was too thick for manual drilling, no significant snow

<sup>\*</sup> AUV track deviated from original route due to strong sub-surface currents

<sup>‡</sup> AUV completed square survey, again slight deviations due to currents



Figure 2: Map of the locations visited during field experiment AS12.

## Chapter 3: Measurements/Results

### 3.1 AUV data

Multibeam sonar data measured by the AUV for floes 1, 2 and 3 of AS12 are presented in figures 3, 4 and 5 respectively. In the case of floe 1 and 3, coverage across the floe is somewhat sporadic, however individual sections have been identified which have reasonable coverage and potentially interesting features.

To remove noise in the data and compensate for its non-uniform spatial distribution, a number of steps were taken to process the data. The data were vertically adjusted a small amount such that a hopefully more accurate sea surface level was represented. Filtering was then performed to remove negative draft values and typically the top 1% of draft values. Finally an interpolation and smoothing process was performed to remove noise, which tended to be in the form of "streaks" in the data. The processed data are presented in figures 6, 7 and 8.

Floe 1 had generally fairly poor data coverage, however three useable sections were identified (1A, 1B and 1C, shown in figure 3). Figure 6 shows 2D and 3D representations of these sections after processing.

The western side of section 1A contains a block or ridge of dimensions of approximately 15 m by 5 m, with depths exceeding 5 m. There is evidence of further thick ice towards the edge of the data coverage to the west and south-west, where drafts are in excess of 3 m. The east of section 1A appears to be comprised of thinner, undeformed ice, generally around 2 m in depth.

Section 1B contains a large, but relatively shallow ridge with drafts of 2-3 m. The rest of the section appears to be comprised of open water or very thin ice, other than one or two smaller ridges or blocks of ice.

The data in section 1C does not show many clearly defined, linear features, however there does appear to be evidence of some deformation and rubble extending to depths of up to 3 m.

Floe 2 contains the most congruous data of all the floes, with a continuous swathe over a roughly 50 m<sup>2</sup> area. The shape of the underside of the stamukha shown in figure 8 appears to be well defined. The draft reaches a depth around 28 m at its maximum, falling to 14 m in the centre of the section before rising again above 25m to the south of the section.

Similar to floe 1, floe 3 contains a large gap in data coverage in its centre. There are, however, a greater number of usable sections of data with features of interest, identified as 3A, 3Bi, 3Bii, 3C and 3D.

Section 3A appears to contain a distinct ridge, however in the centre of this ridge are patches of anomalously low draft values and missing data, which draws into question the reliability of the data within this section. If accurate, the data suggests that the ridge is fairly large and peaks at a draft of 6

m. The west edge of the section is dominated by thicker, deformed ice, while the ice to the east of the section is much thinner.

Section 3B is comprised of two sections (3Bi and 3Bii). These sections both contain ridges or blocks which might both belong to one continuous, linear feature. The ridge in section 3Bi extends to depths of around 5 m, however it is not perfectly linear and appears to be made of a number of smaller blocks. While the ridge in 3Bii is of a similar depth, it is more clearly linear and symmetrical than the ridge in 3Bi. The sides of the ridge in 3Bii are also steeper, so much so that they may be an artifact of "streaks" in the unprocessed data, most of which were removed in the smoothing process.

Section 3C appears to contain a number of small blocks, with a maximum depth of around 3 m. Together, these blocks form part of a rubble field. There is some evidence of a linear feature through the centre of this section, including the two largest blocks and a lead to the south of this. If this is the case then the feature has clearly been heavily eroded.

Section 3D still shows some strong signs of the previously mentioned "streaks" in the data, which could not be removed without excessive smoothing. Despite this, it is still possible to make out some features, such as the large mass of ice 3.5 to 4 m thick in the south west of the section and two to three smaller, blocky features in the centre of the section, which have drafts up to 3.5 m.

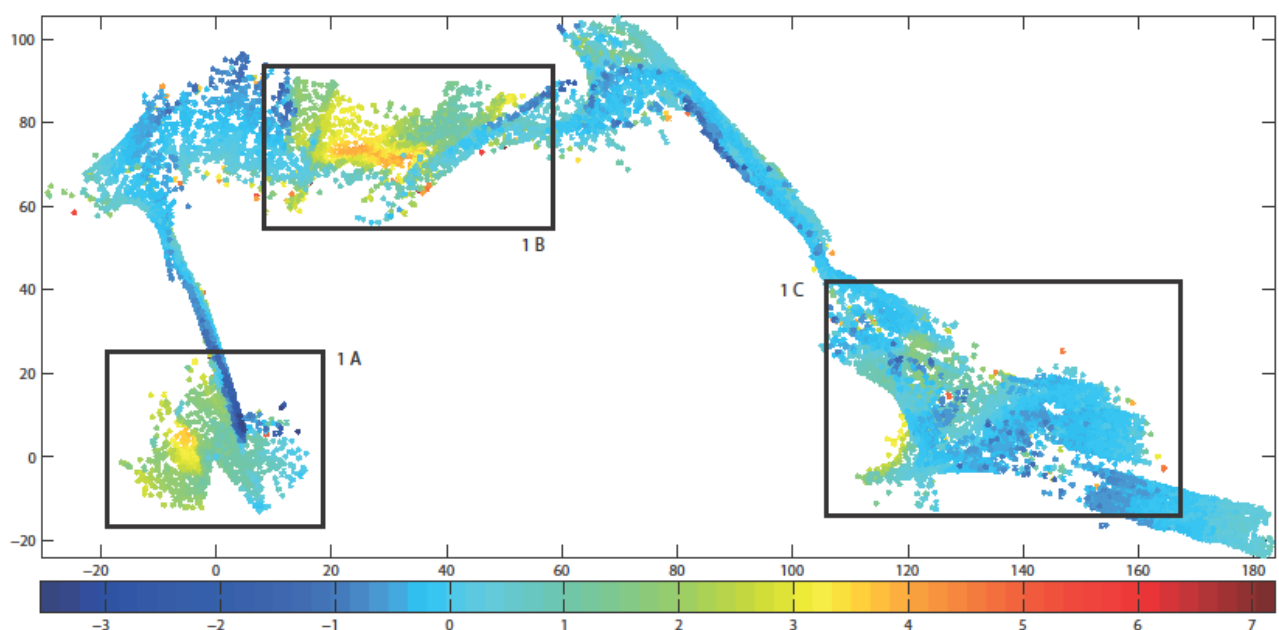


Figure 3: Map showing the unprocessed multibeam AUV data from floe 1 of AS12. The x and y axes are in metres and the colour bar represents draft in metres. The subsections of the floe analysed in greater details are outlined by black boxes.

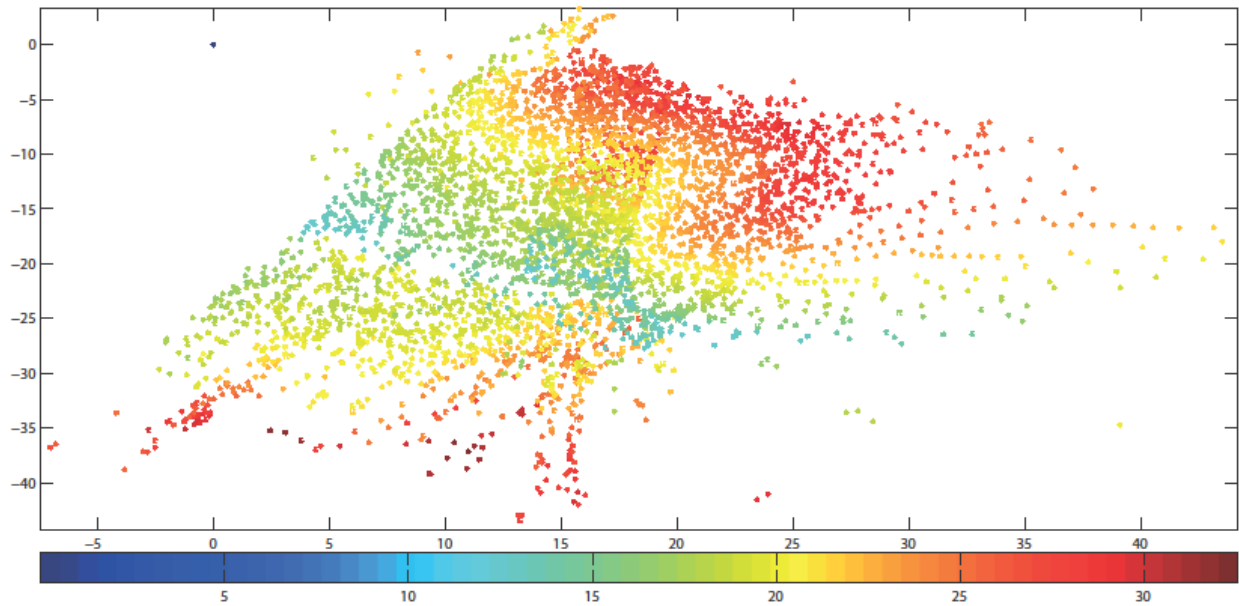


Figure 4: Map showing the unprocessed multibeam AUV data from floe 2 of AS12. The x and y axes are in metres and the colour bar represents draft in metres.

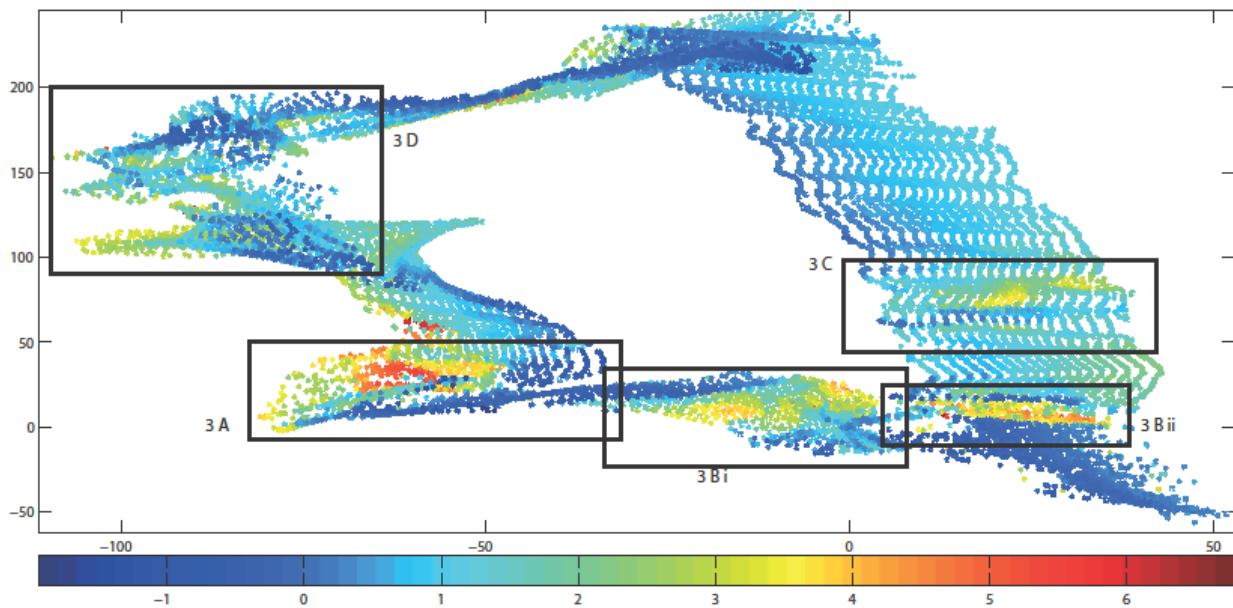


Figure 5: Map showing the unprocessed multibeam AUV data from floe 3 of AS12. The x and y axes are in metres and the colour bar represents draft in metres. The subsections of the floe analysed in greater details are outlined by black boxes.

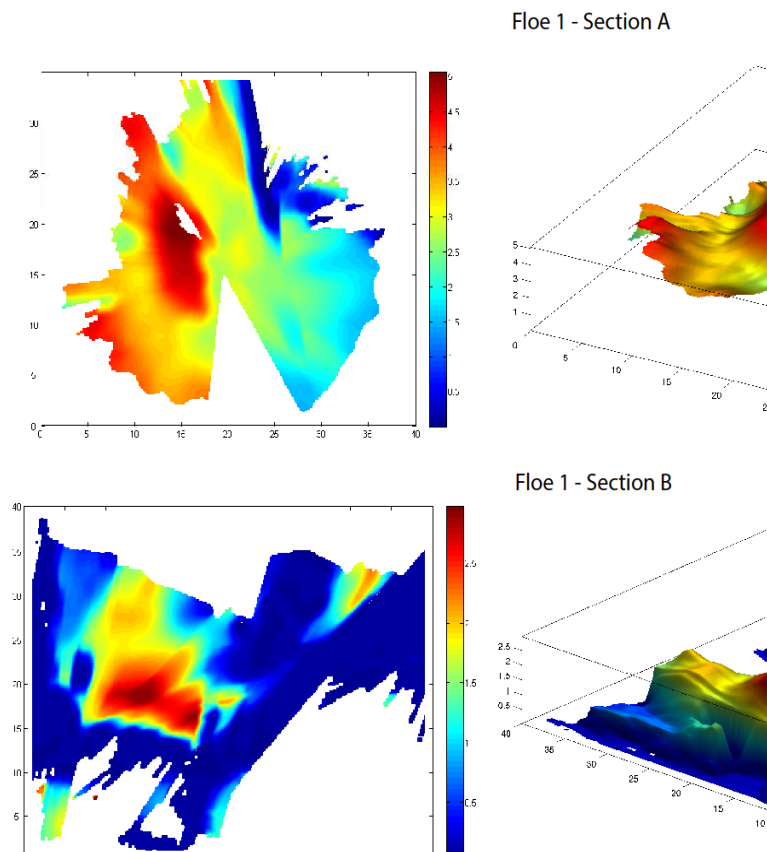
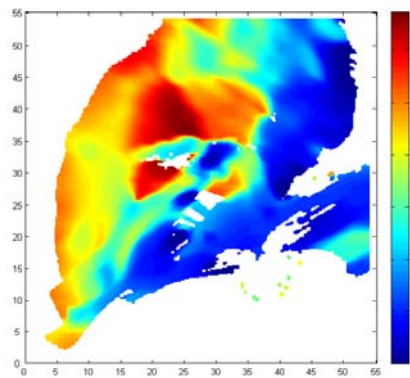
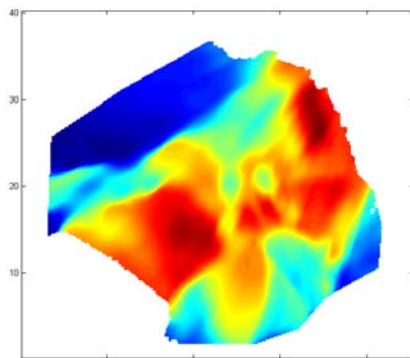
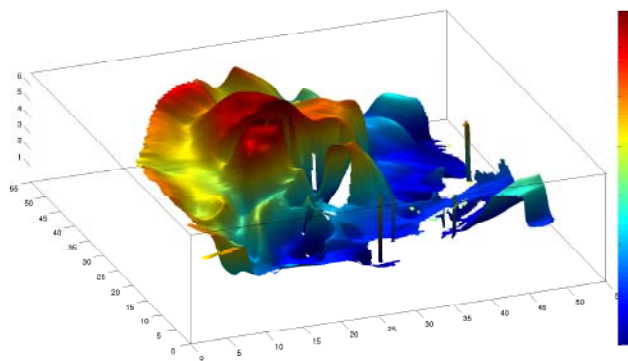


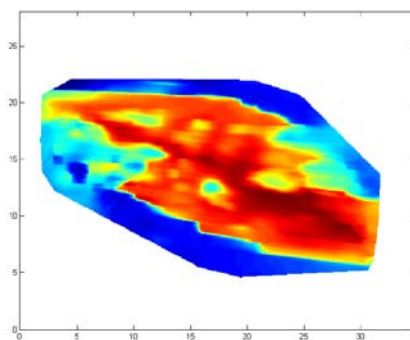
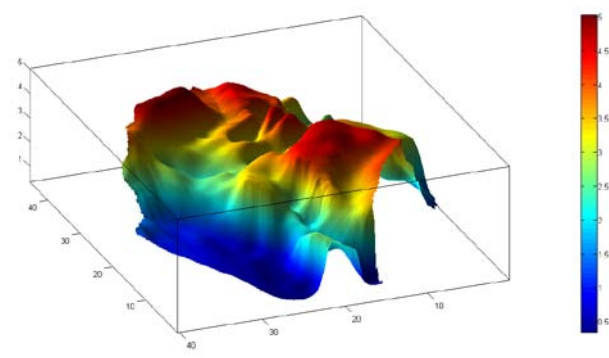
Figure 6: Multibeam AUV data from floe 1 of AS12. 2D and 3D representations are given. The x and y axes are in metres. The z axis and colour bar represent draft (inverted for 3D plots) in metres.



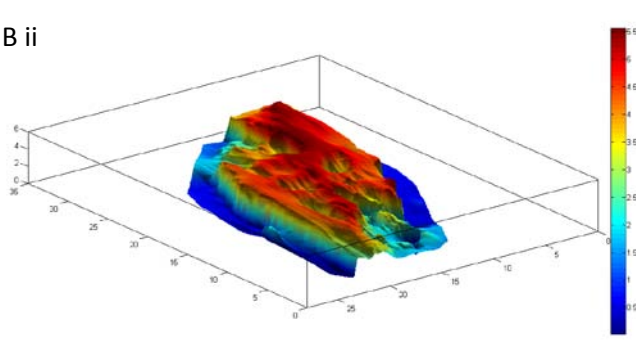
3 A



3 B i



3 B ii



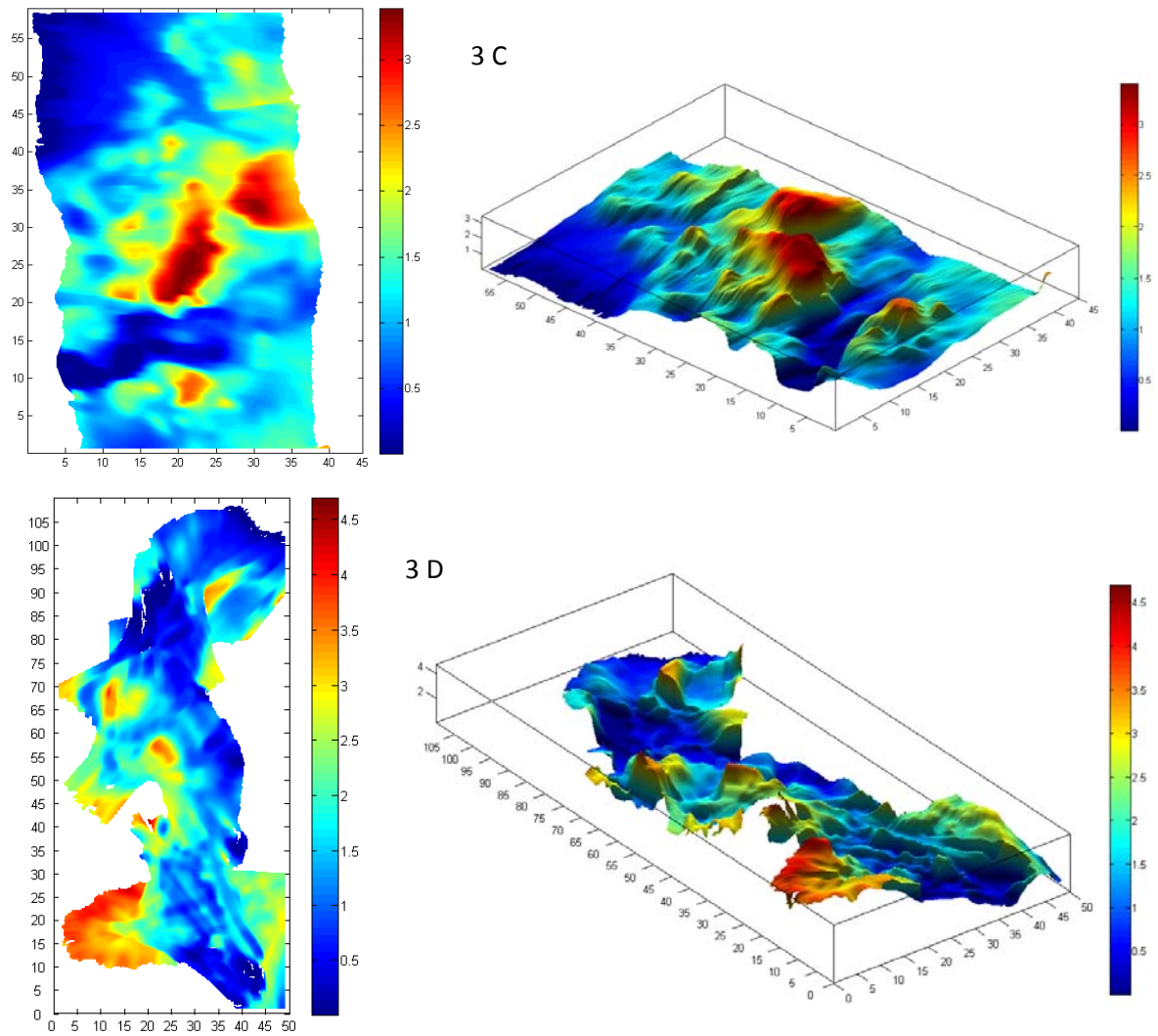


Figure 7: Multibeam AUV data from floe 3 of AS12. 2D and 3D representations are given. The x and y axes are in metres. The z axis and colour bar represent draft (inverted for 3D plots) in metres.

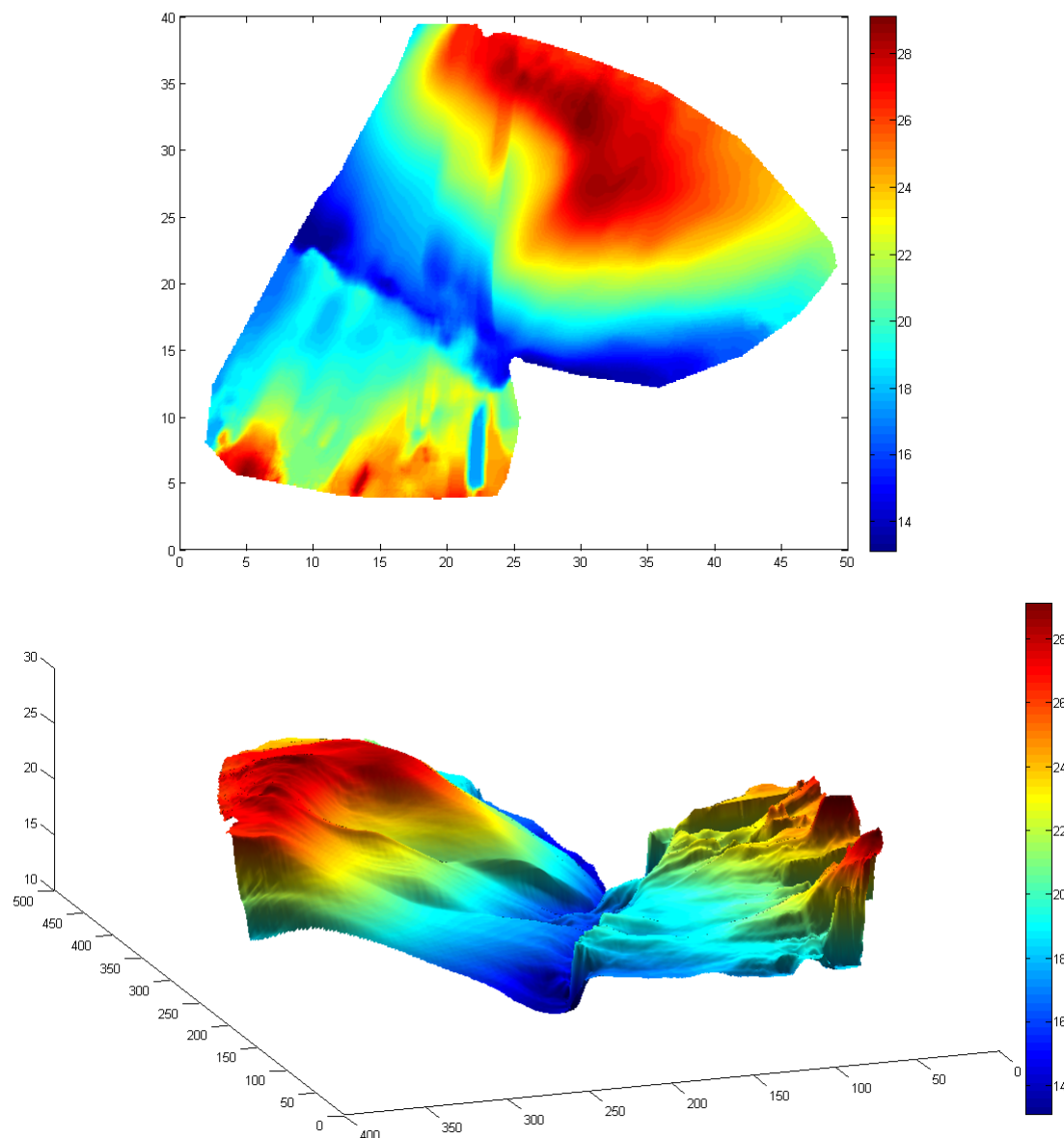


Figure 8: Multibeam AUV data from floe 2 of AS12. 2D and 3D representations are given. The x and y axes are in metres. The z axis and colour bar represent draft (inverted for 3D plots) in metres.

### 3.2 LiDAR

In an Arctic first, 3D scanning experts worked with sea ice scientists in situ to make the best use of state-of-the-art laser technology. The 3D replica of the ice surface produced provides information on pressure ridge topography and melt pond sizes and shapes as well as snow drift patterns and individual ice block characteristics.

In total, 10 floes were scanned as a part of AS11 and 5 more during AS12. An overview of these scans is presented in figure 9. Data from the scans of the AS12 floes is shown in figures 10 and 11. A number of features are visible in figure 10, including ridges, rubble and leads. The topography of the stamukha is also well captured in figure 11. An example of how different ice morphologies can be

differentiated using the LiDAR data is included in figure 12, as are probability density functions of the freeboard for each morphology identified.

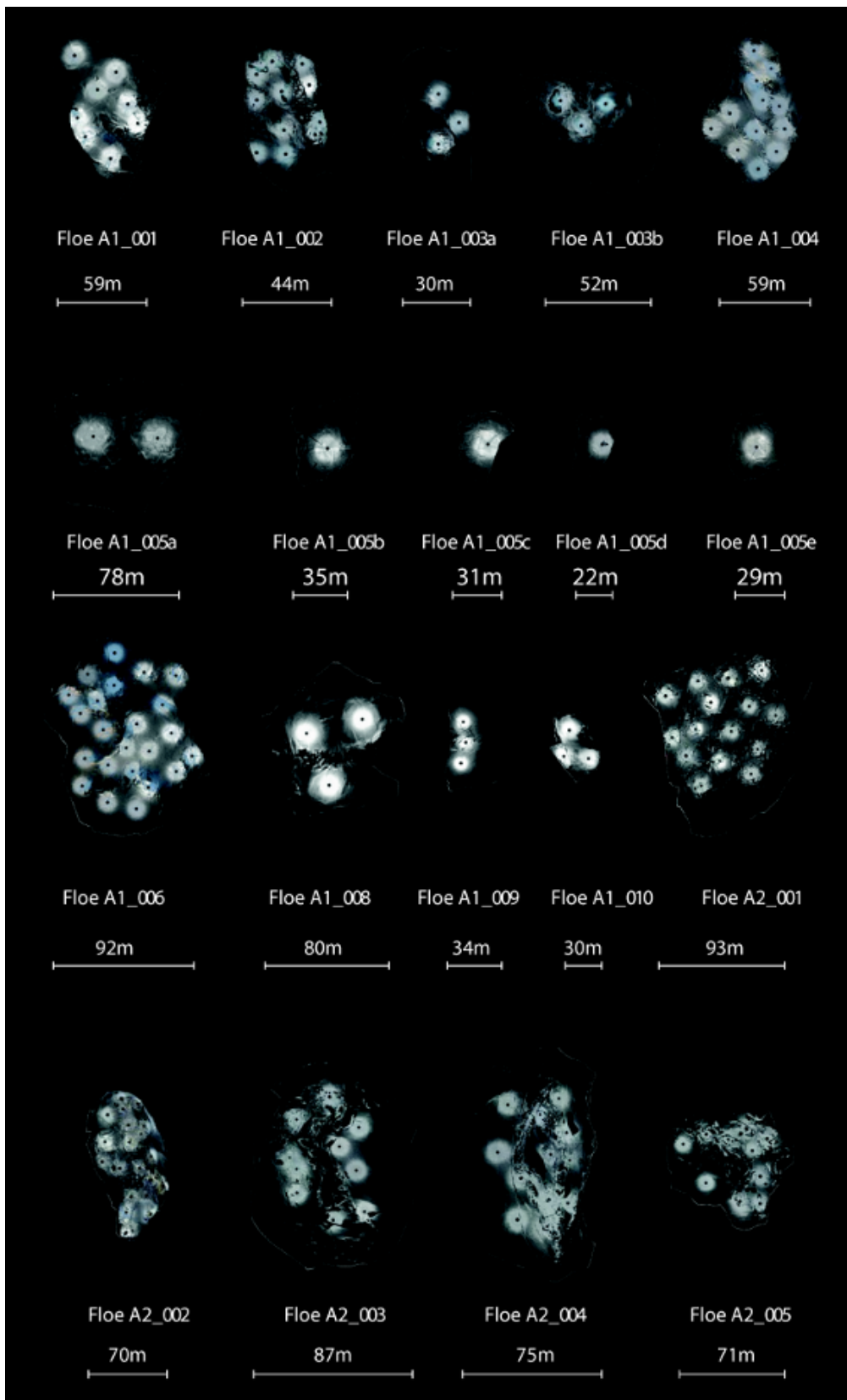


Figure 9: Overview of all ice floes scanned using 3D LiDAR technology during the SIDARUS-1 and SIDARUS-2 campaigns.

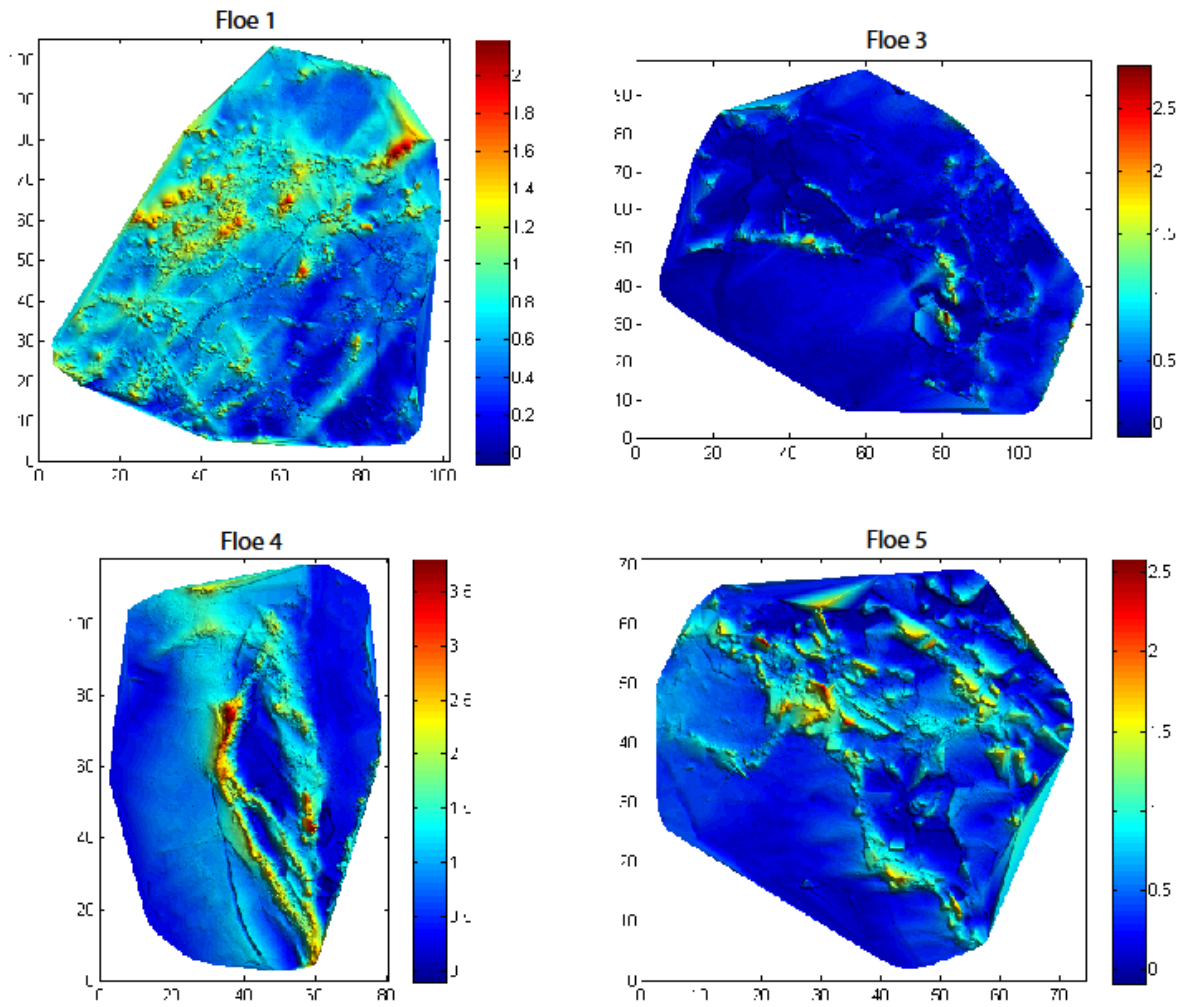


Figure 10: LiDAR data from floes 1, 3, 4 and 5 of AS12. The x and y axes are in metres. The z axis and colour bar represent freeboard in metres.

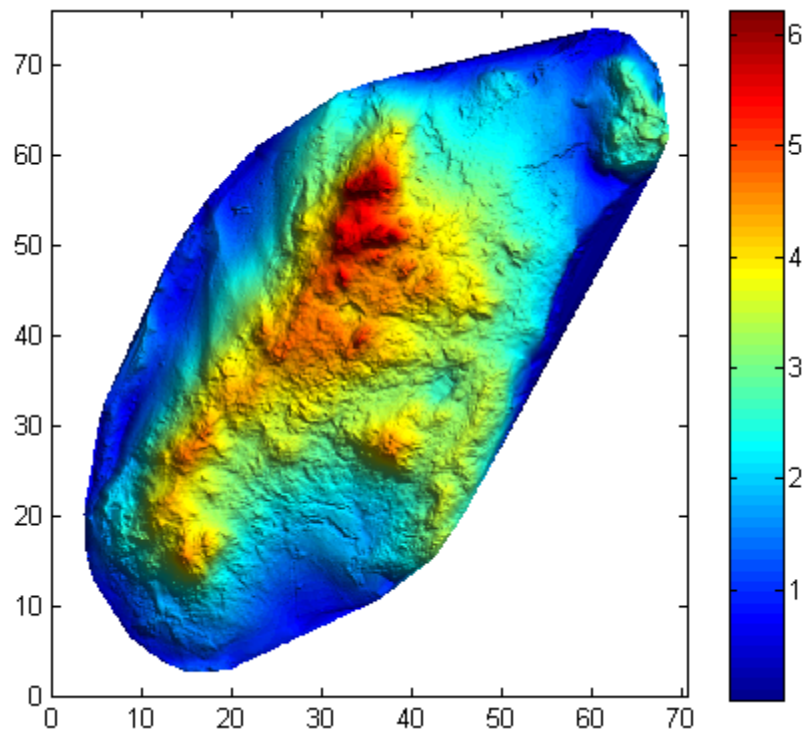


Figure 11: LiDAR data from floe 2 of AS12. The x and y axes are in metres. The z axis and colour bar represent freeboard in metres.

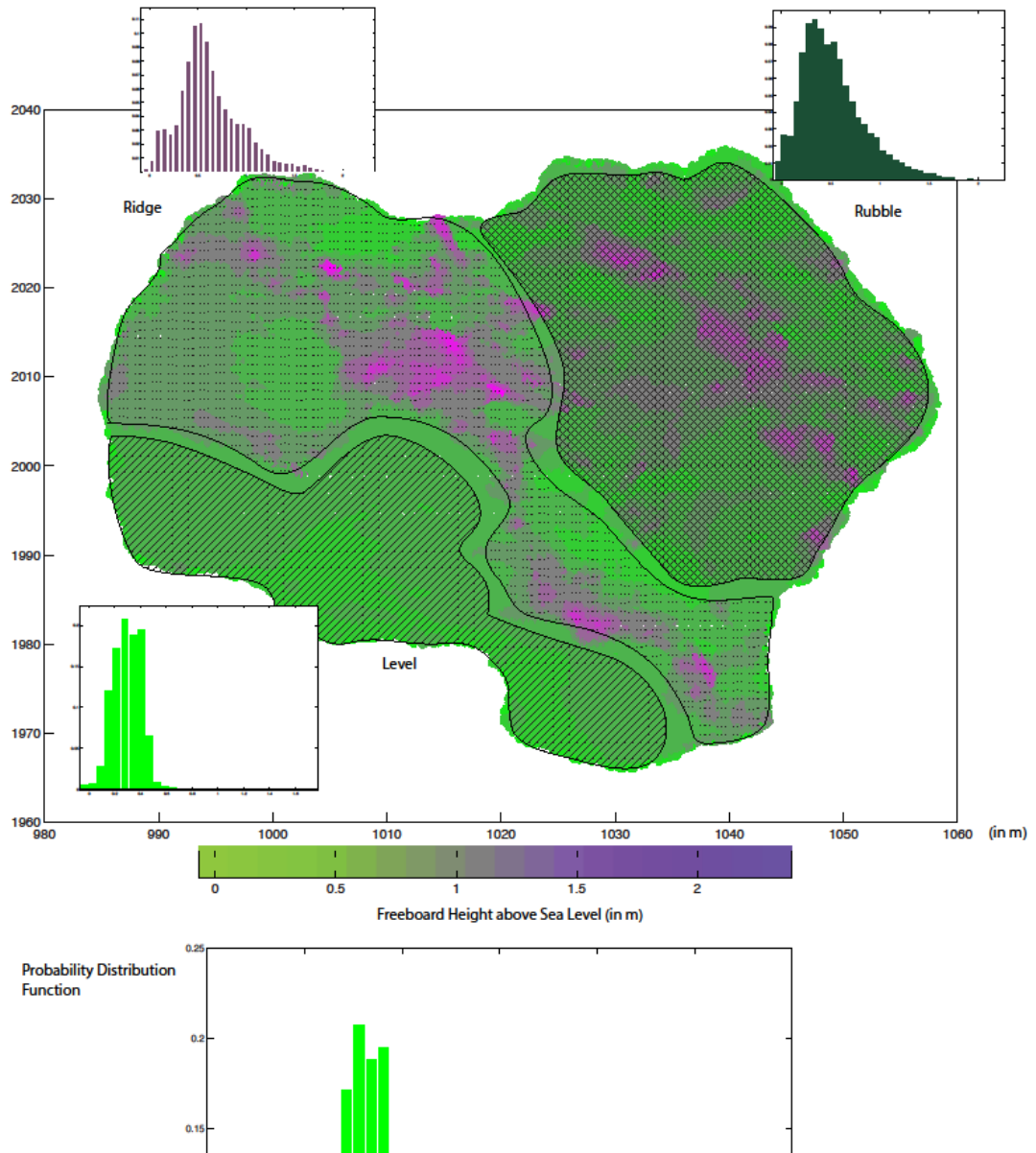


Figure 12: LiDAR scan of surface structure of floe 5 from AS12. Visually distinguishing three types of ice morphology (level, ridged, rubble) and probability density functions for the freeboard of for all three.

### 3.3 Drill lines

To obtain a comprehensive idea of the whole structure of the ice floe it is necessary to not only measure its surface but also the snow cover and thickness in greatest possible detail. The different data sets (scans, snow and thickness) can then be tied together by means of a survey station, a typical output of which is seen on the right. As September is at the end of the melt season, there is rarely significant snow found on sea ice in the Arctic. The measured ice thicknesses varied greatly depending on whether the floe consisted of first year ice or multiyear ice. For first year ice, average thicknesses were usually around 1-2 m, whereas the older, more deformed, multiyear ice featured average thicknesses up to 4 m.

Scatter plots relating floe thickness and freeboard measurements are shown in figure 13 (for AS11) and figure 14 (for AS12). A positive correlation between freeboard and thickness was found in both cases. Figure 15 illustrates a compilation of the draft, freeboard and snow measurements for one drill line. Similar figures are included in the appendix, showing freeboard and draft profiles for all the drill lines taken in AS11.

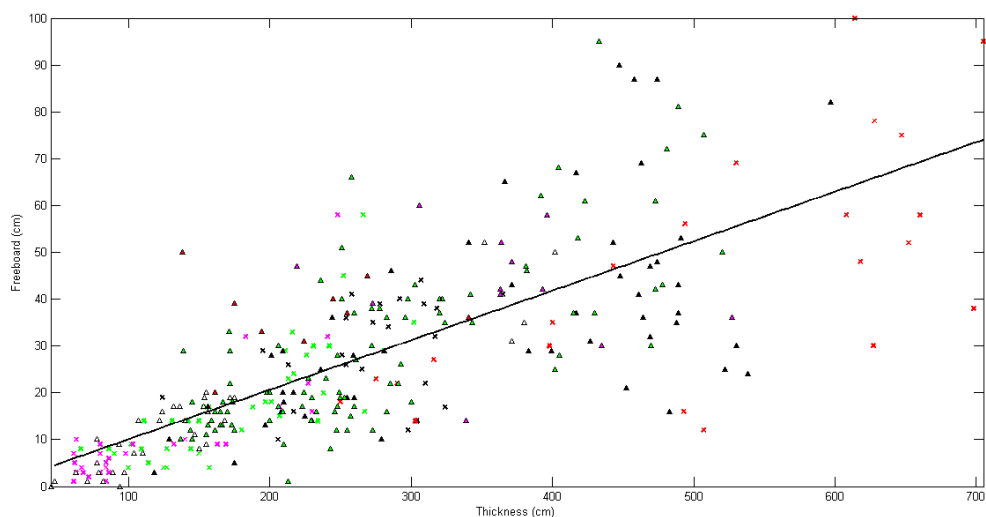


Figure 13: Scatter plot of floe freeboard vs. thickness for AS11 campaign. Each marker represents one of 9 different floes. There are 347 data points in total. Y-intercept: -0.5018 cm, slope: 0.1058, correlation coefficient: 0.7535.

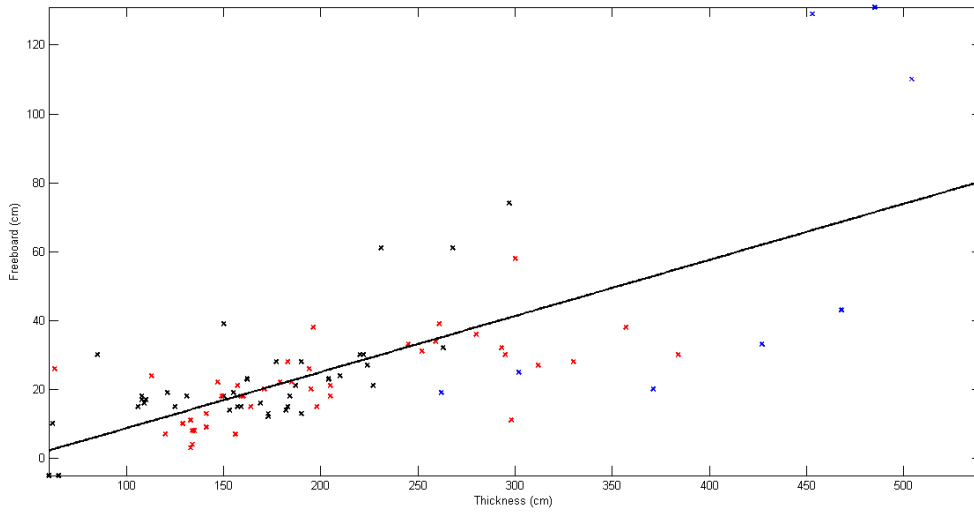


Figure 14: Scatter plot of floe freeboard vs. thickness for AS12 campaign. Each marker represents one of 3 different floes. There are 89 data points in total. Y-intercept: -7.6078 cm, slope: 0.1629, correlation coefficient: 0.7267.

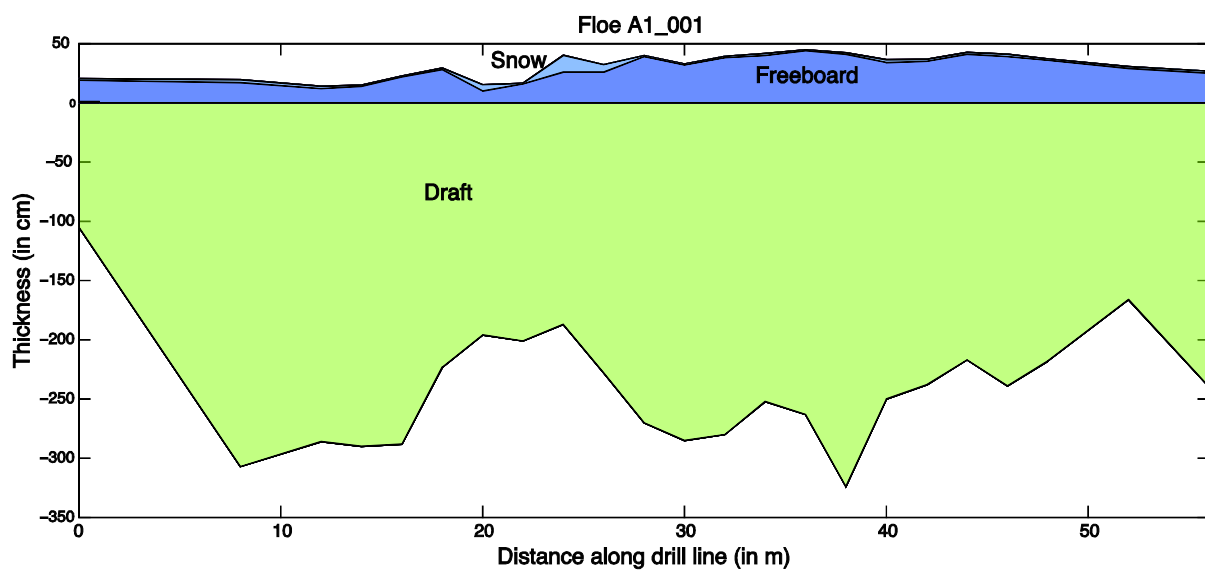


Figure 15: Example of a drill line plus snow depth measurements.

### 3.4 Aerial imaging

Grids and line patterns were own by the helicopter, enabling large scale aerial imagery surveying of the conditions in the local MIZ (survey areas: 1 - 50 nm<sup>2</sup>). This will allow us to extract statistics like floe sizes (as function of distance to ice edge), preferred break up orientation, ridge frequencies and directions. The aerial photographs collected play an important role in providing a mesoscale that links the small scale results gained from studying individual floes to the basin wide surveys performed by satellite data. Comparing floe scans to aerial grids for example gives insights into how local ridge conditions affect the floe distribution over a larger area. This in turn provides information as to how to interpret data with much bigger footprints from satellite radars.

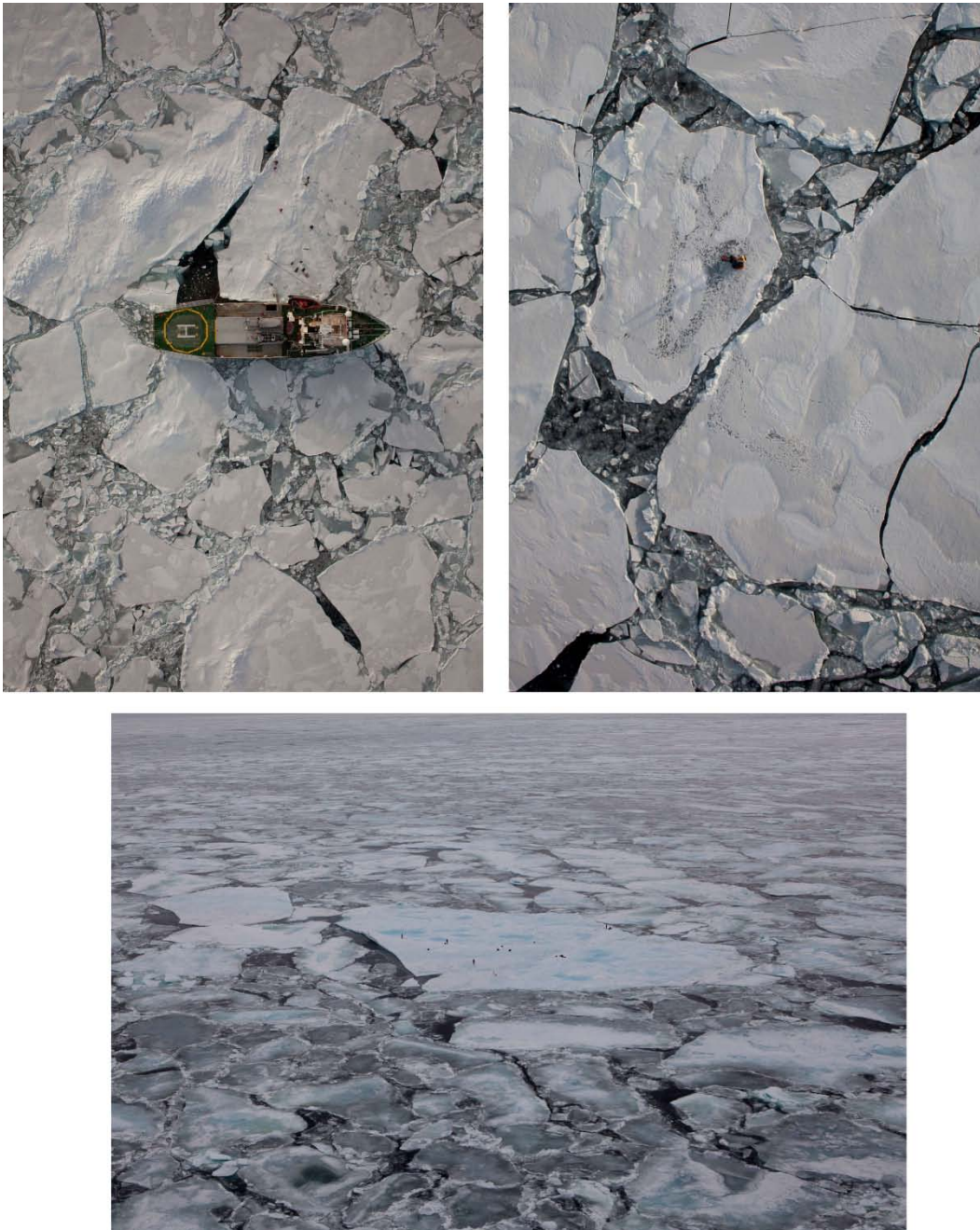


Figure 16: Aerial images of three of the floes surveyed during AS11 (clockwise from top left): A1\_002; floes A1\_005d (with 3 scientists) and A1\_005e (adjacent to 5d bottom right); floe A1\_003a and A1\_003b (before breakup); Photographs: Nick Cobbing/Greenpeace

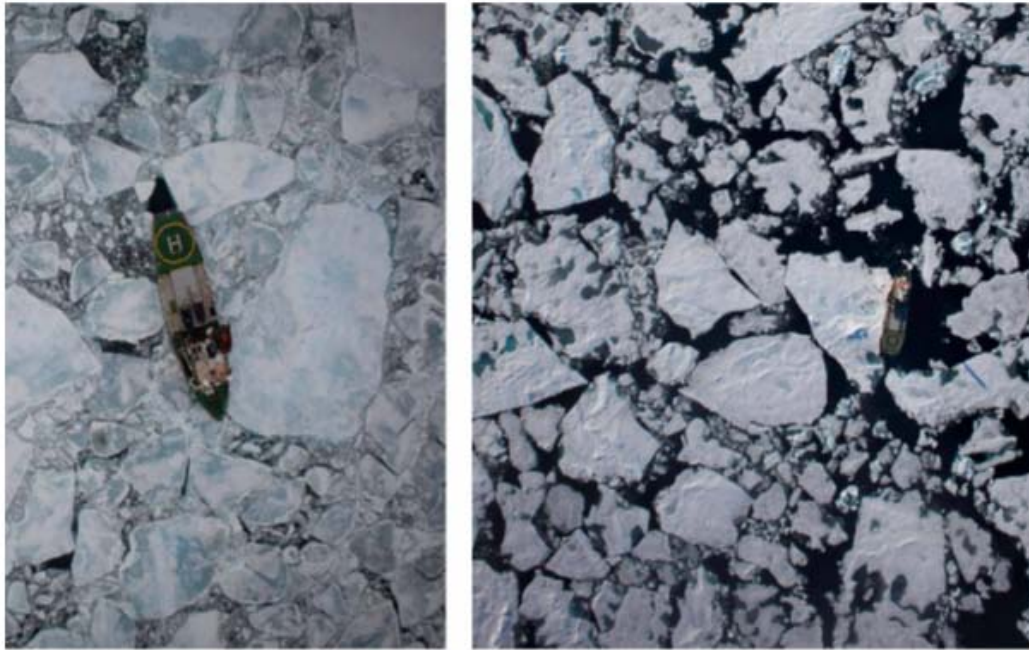


Figure 17: Aerial images of two of the floes surveyed during AS11: A1\_004 (left); A1\_001 (right); Photographs: Nick Cobbing/Greenpeace

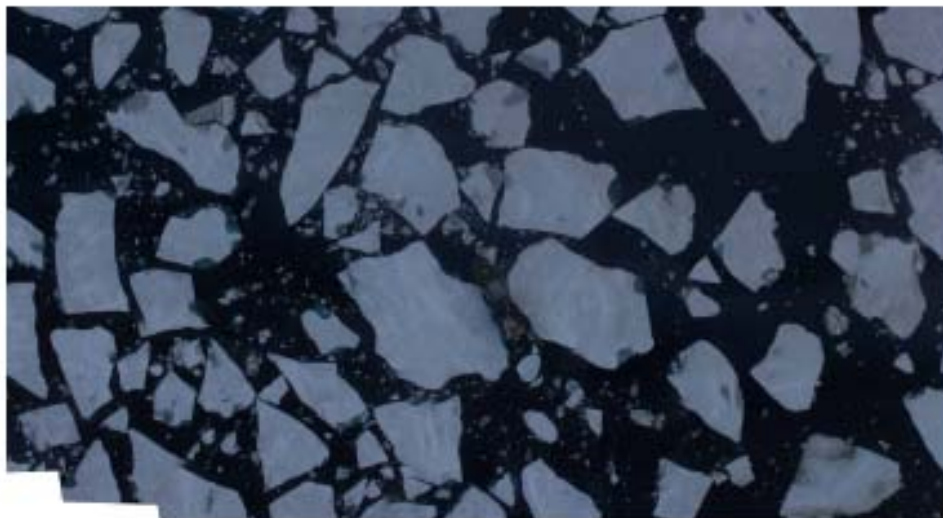


Figure 18: Example aerial image obtained through AS11, the mosaicked image consists of 15 individual images (for scale the Arctic Sunrise can be seen in the center of the image).

## Chapter 4: Discussion

### 4.1 AUV

The multibeam sonar data from the AUV suffered from two major issues. The first was the incomplete coverage of the floes. This may have been due to currents which prevented the AUV from following its preferred course. This prevented a complete characterisation of the underside of floes 1 and 3 being performed. The second is the presence of “streaks” in the data. These streaks were largely smoothed out during the processing of the data, however they remain present in some sections even after smoothing. Balancing the amount of smoothing performed such that the noise was reduced, but also such that the shape of major features could be resolved lead to a radius of smoothing of approximately 0.5 m being used on the data.

The issues associated with the data from the AUV limits attempts to collocate and compare AUV and LiDAR data, with identifying and aligning subsurface features with surface features posing an ongoing challenge which we continue to work on. However, for the stamukha in floe 2 of AS12, adequate AUV coverage has allowed for collocation with LiDAR to be attempted. Figure 19 shows the results of this attempt, where the peak draft values recorded by the AUV were aligned with the peak freeboard values from the LiDAR data.

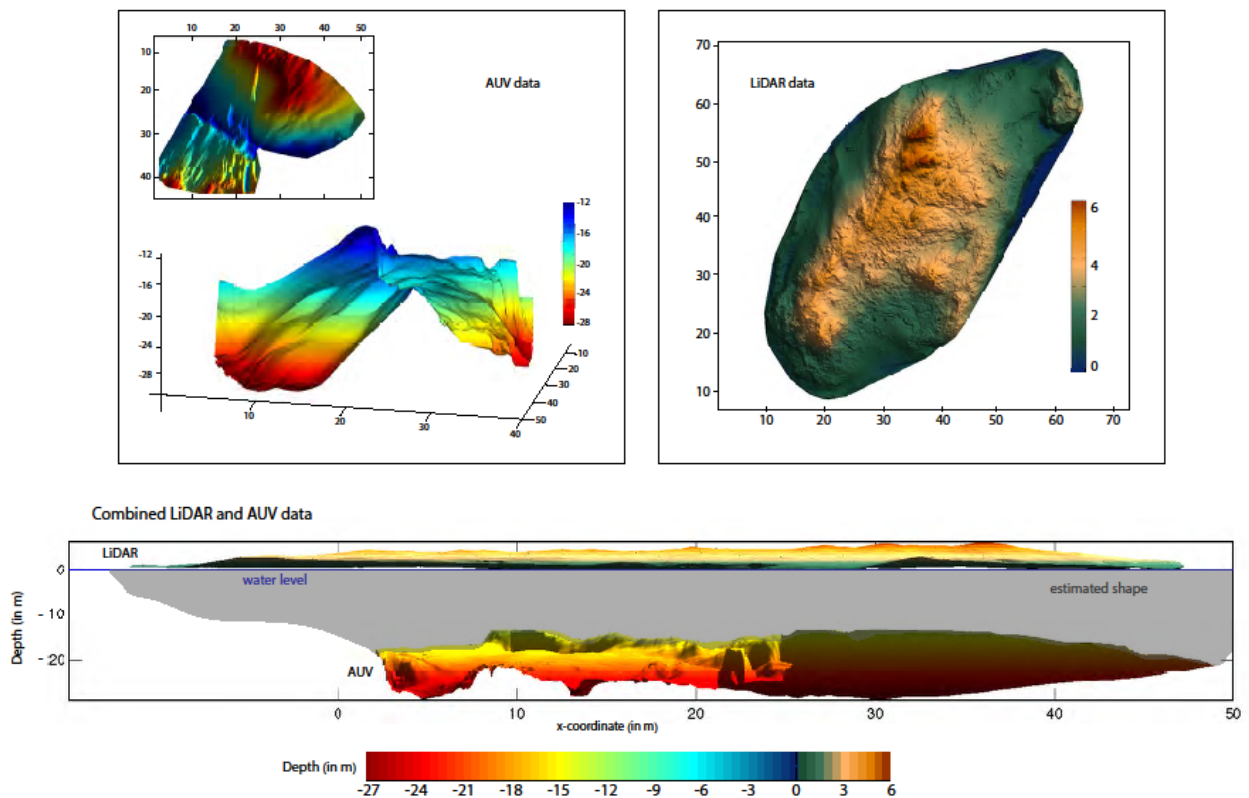


Figure 19: Collocated AUV and LiDAR data for the stamukha in floe 2 of AS12.

## 4.2 LiDAR

Probability density functions were generated for the data from floes 1-4 of AS12. The shapes of these PDFs reflect the morphology of the ice in each floe. For example, the more deformed floes from figures 10 and 11 (floe 1 and 2) are clearly distinguishable from the less deformed floe (3) by their wider spread of values and higher averages. For figure 4, two distinct floes are identifiable by the separate peaks in the PDF, suggesting a combination of more and less deformed ice.

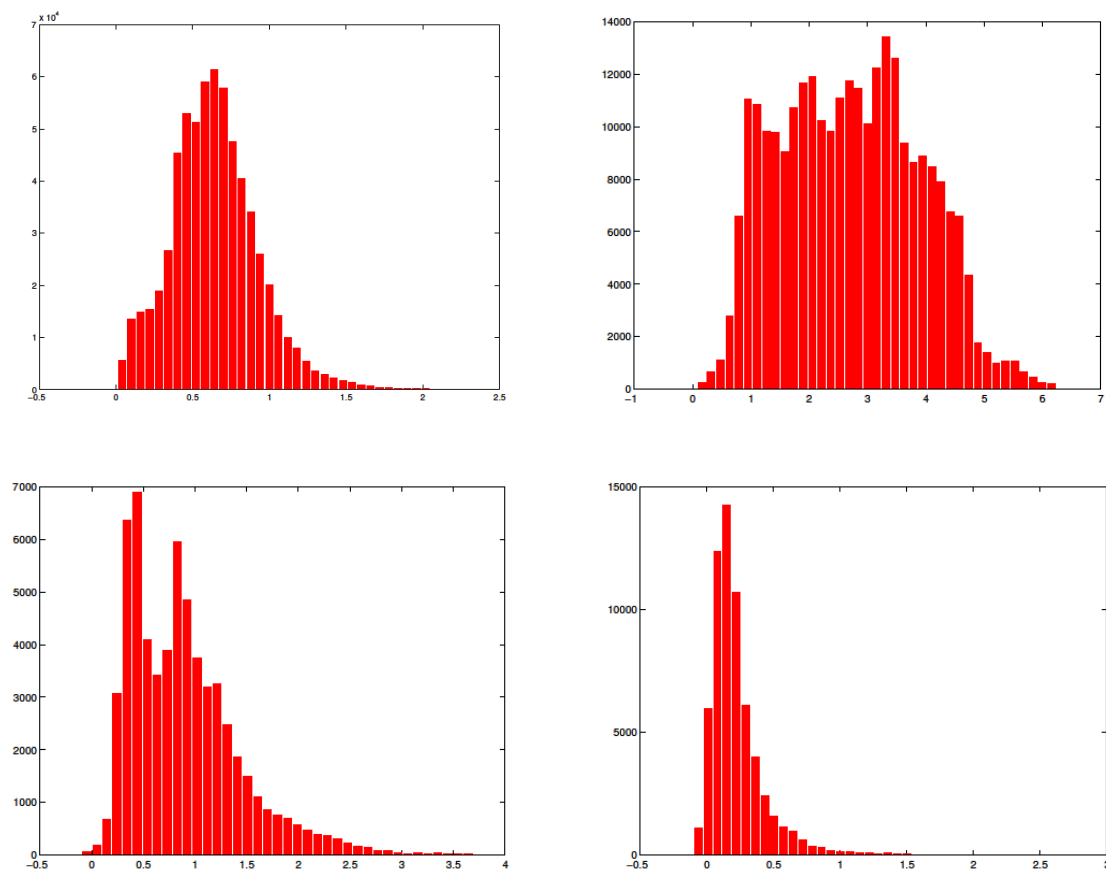


Figure 20: PDFs of LiDAR scans of surface structure of AS12 floes 1 to 4- see figures 10 and 11. Note the clearly distinguishable PDF shapes for different types of ice (clockwise from top left): multi-year 'rubble' ice, smoothed PDF with freeboard up to 2 m; top hat shaped PDF for the Stamukha, representing the constant gradient of the conically shaped surface; narrow PDF for a level first year ice floe; two-peaked PDF for two floes of different thickness rafted - compare the surface plots of figure 8.

### 4.3 Drill data

The observed relationships between ice freeboard and thickness values for AS11 and AS12 are shown in figures 13 and 14. Least squares regression lines for these data were calculated, the slope of which suggests the following relationships between ice freeboard and thickness:

$$\text{AS11: } F = 0.1058 \times H$$

$$\text{AS12: } F = 0.1629 \times H$$

, where F is the freeboard elevation, H is the ice thickness and, assuming isostatic equilibrium, 0.1058 and 0.1629 are equal to:

$$1 - \frac{\rho_{ice}}{\rho_{water}}$$

The high correlation coefficients for the data, combined with a y intercepts close to zero, support the validity of this relationships. The slope values for this relationship are in good agreement with other similar estimates (0.106 from Alexandrov et al., 2010 and 0.111 from Wadhams 1992, 2000). The average density of the sea ice estimated from these relationships are 918 kg m<sup>-3</sup> for AS11 and 860 kg m<sup>-3</sup> for AS12, which are within the range of measured densities reported in the literature (e.g. 750 to 960 kg m<sup>-3</sup> for first year and 720 to 940 kg m<sup>-3</sup> for multiyear ice, Timco and Frederking, 1996).

From the above relationship, it can be inferred that the greater the slope, the lower the density of the ice relative to the water. Variations in the slope value could therefore be used as a proxy for differentiating ice regimes, as multiyear ice is generally of lower density as a result of fewer voids and lower salinity, therefore resulting in greater slopes. This has also been suggested by Ackley et al. (1974) who stated that higher freeboards lead to lower average densities after work on ice profiles on AIDJEX stations.

Floes 1, 2, 3, 6, 9, 10 and line 7D were identified as being deformed floes, while lines B-E for floe 5 and lines A-C for floe 7 were identified as being undeformed floes. The observed relationship between freeboard and thickness for deformed and undeformed floes is shown in figure 21. Counter to what would be expected, a greater slope was observed for undeformed floes than deformed floes. A number of possible explanations exist for this. Firstly, while multiyear ice is generally of a lower density than first year ice, large variations in the densities of both types of floe have been observed and the results may be unrepresentative of these floe types in general. There is also the possibility that differences in snow cover over both floe types may influence the freeboard to thickness

relationships. It is also likely that pointwise isostatic equilibrium is not a reliable assumption, which combined with a possible systematic bias introduced by not drilling directly through the sails of the floes could explain the unexpected results.

It is also worth mentioning that the data does not appear to show distinct cut-offs between deformed and undeformed floes. Instead, the data imply more of a continuum of deformity.

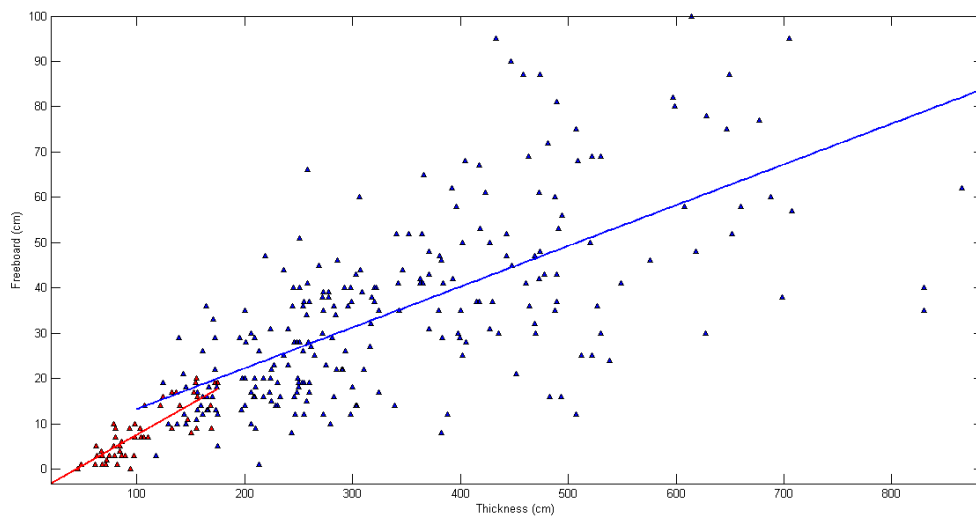
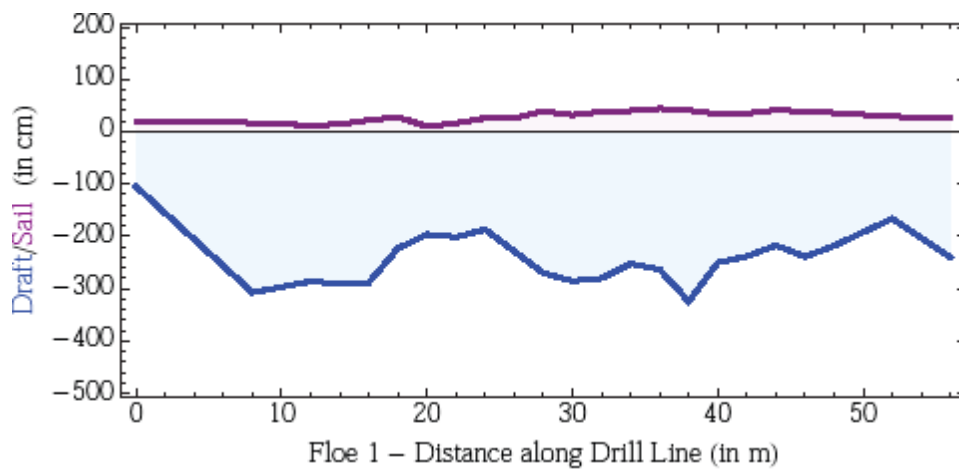


Figure 21: Scatter plot of floe freeboard vs. thickness for AS11 campaign. Blue triangles represent data from deformed floes and red triangles represent data from undeformed floes. There are 351 data points for deformed floes and 53 data points for undeformed floes.

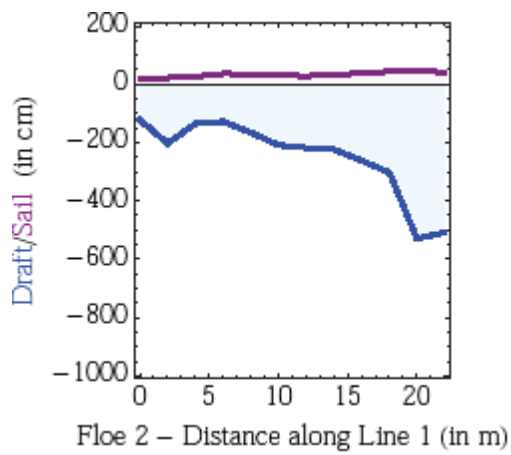
For deformed floes: Y-intercept: 4.2740 cm, slope: 0.0900, correlation coefficient: 0.6561.

For undeformed floes: Y-intercept: -5.8763 cm, slope: 0.1348, correlation coefficient: 0.8299.

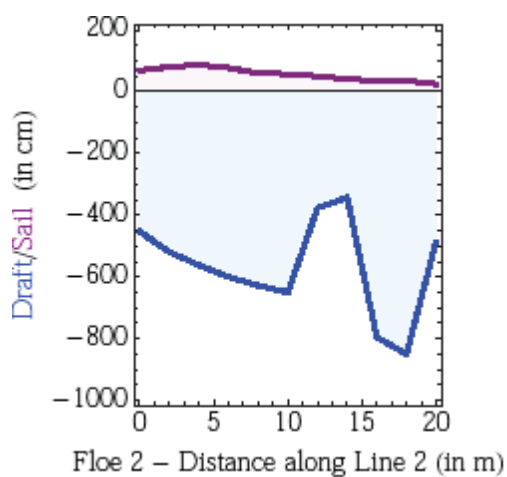
## Chapter 5: Appendix: AS11 drill line profiles



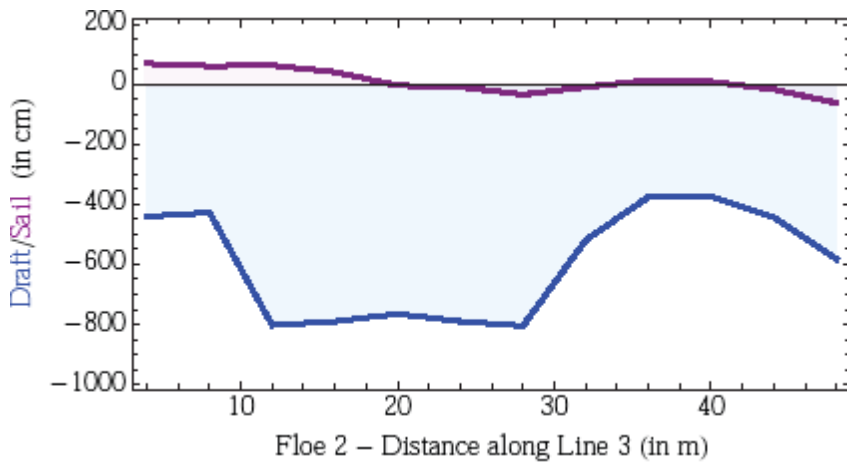
Floe 1 ALine



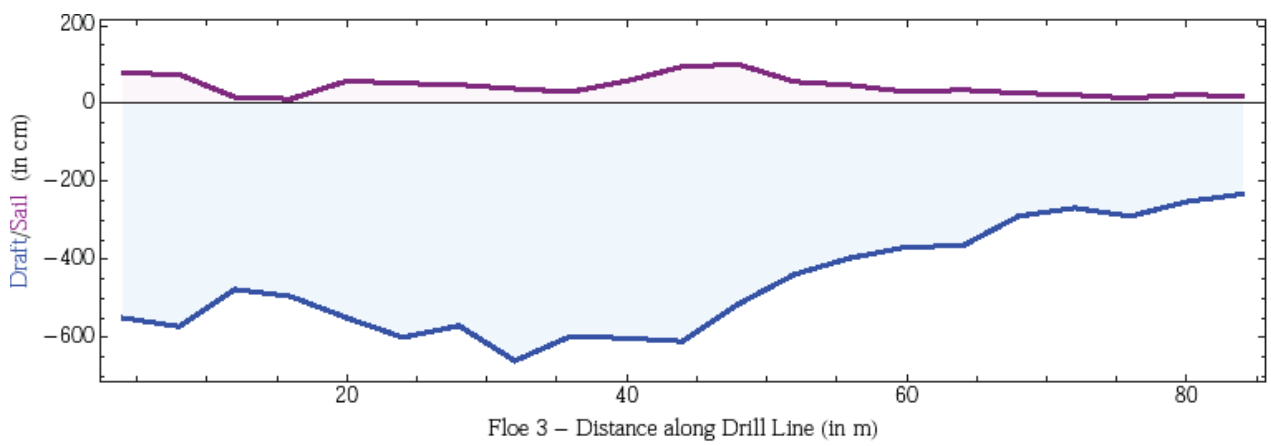
Floe 2 ALine



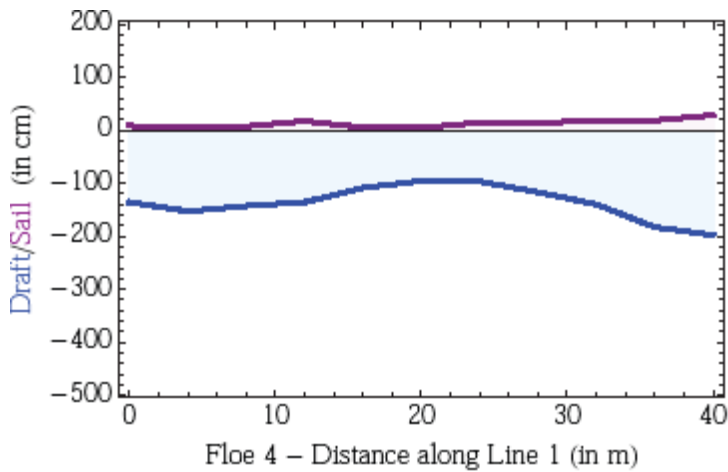
Floe 2 BLine



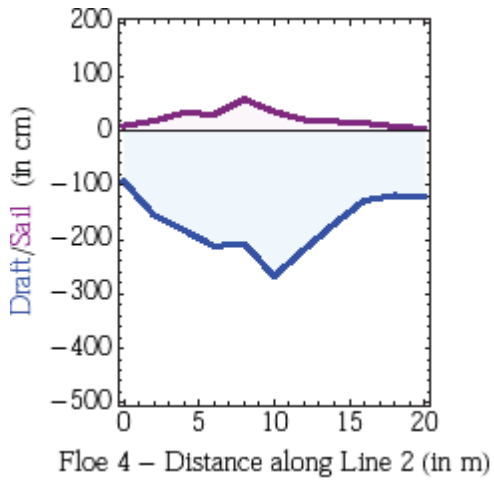
Floe 2 CLine



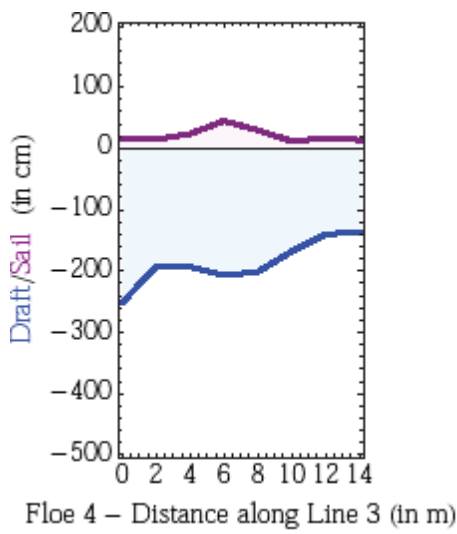
Floe 3 ALine



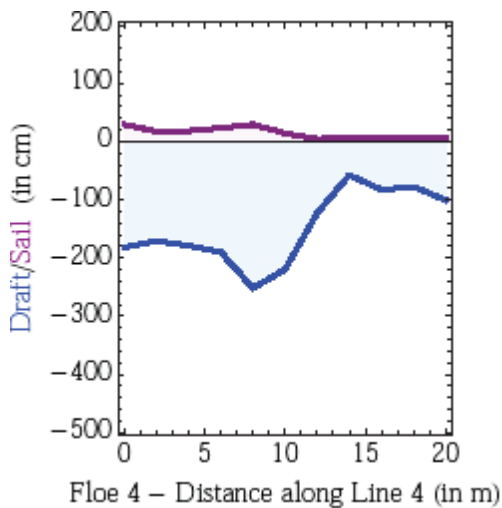
Floe 4 ALine



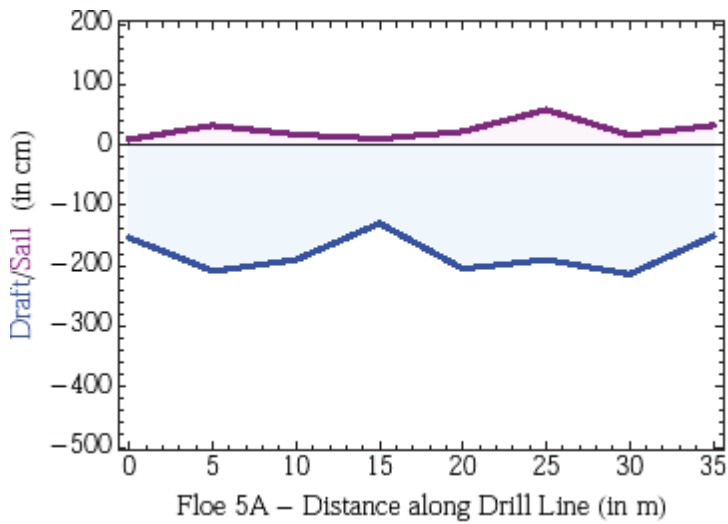
Floe 4 BLine



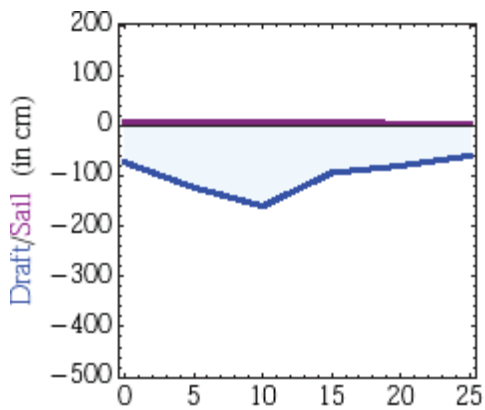
Floe 4 CLine



Floe 4 DLine

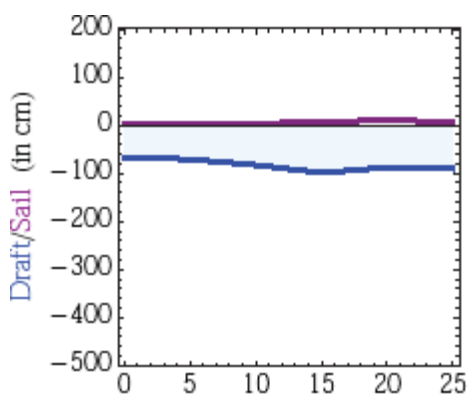


Floe 5A



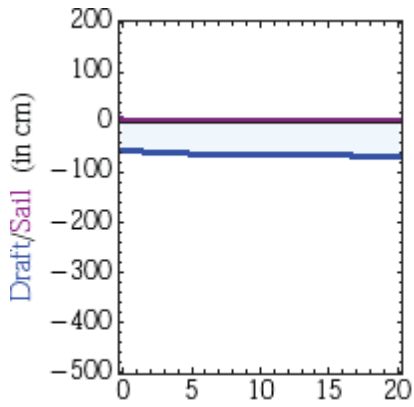
Floe 5B – Distance along Drill Line (in m)

Floe 5B



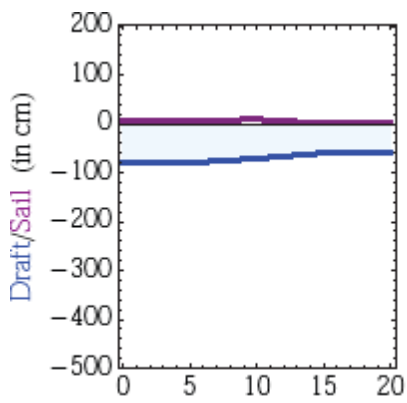
Floe 5C – Distance along Drill Line (in m)

Floe 5C



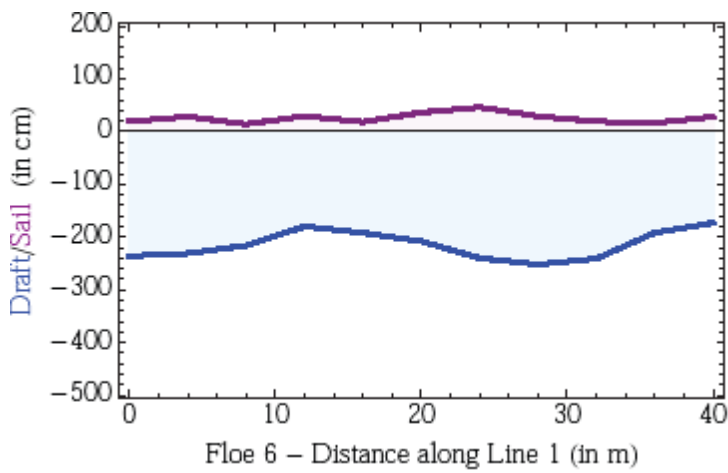
Floe 5D – Distance along Drill Line (in m)

Floe 5D

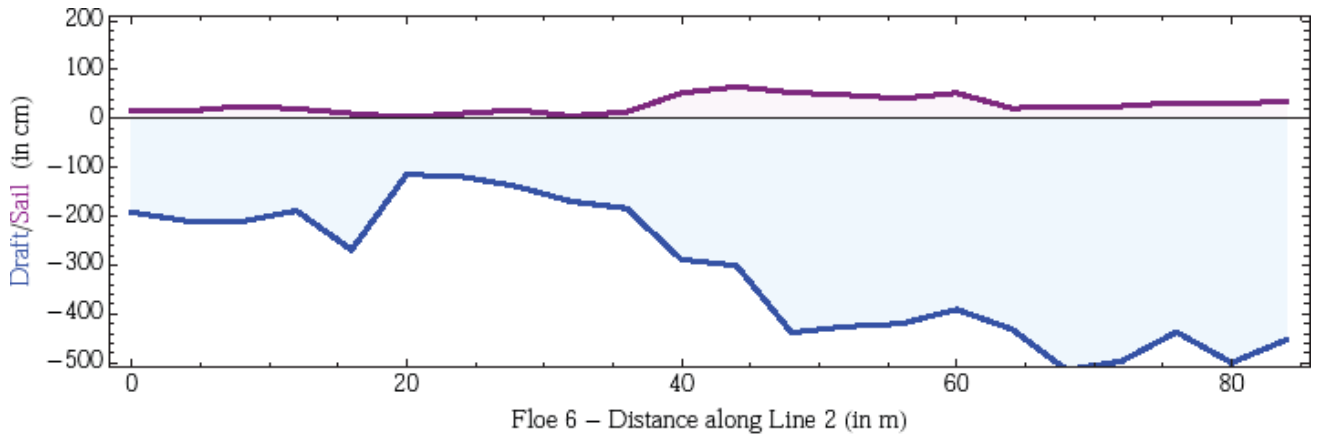


Floe 5E – Distance along Drill Line (in m)

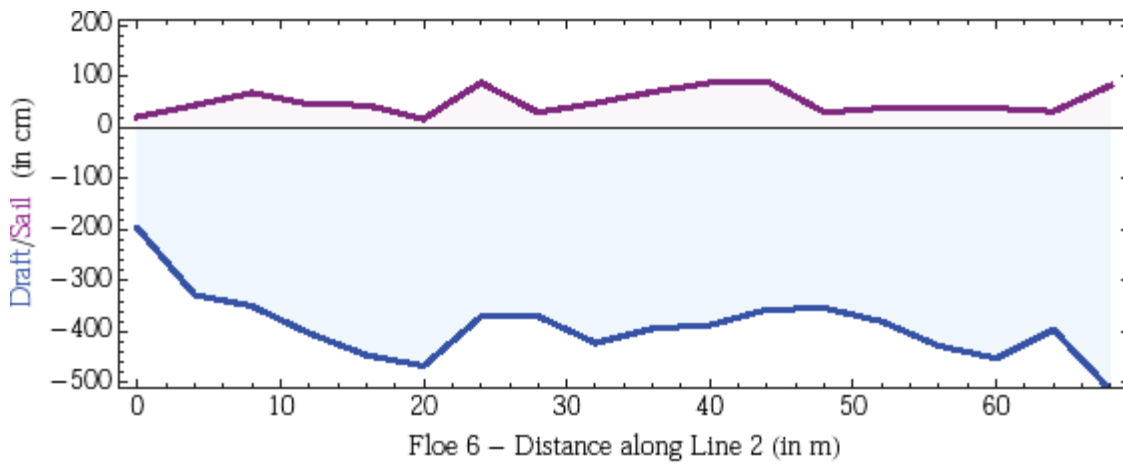
Floe 5E



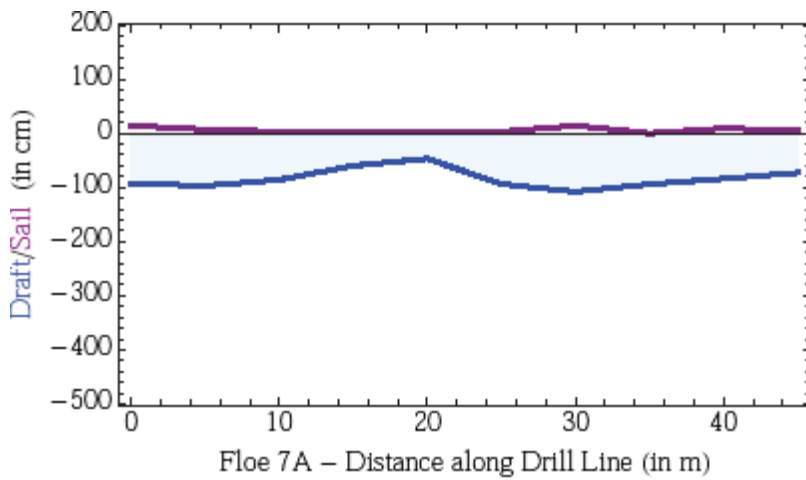
Floe 6 ALine



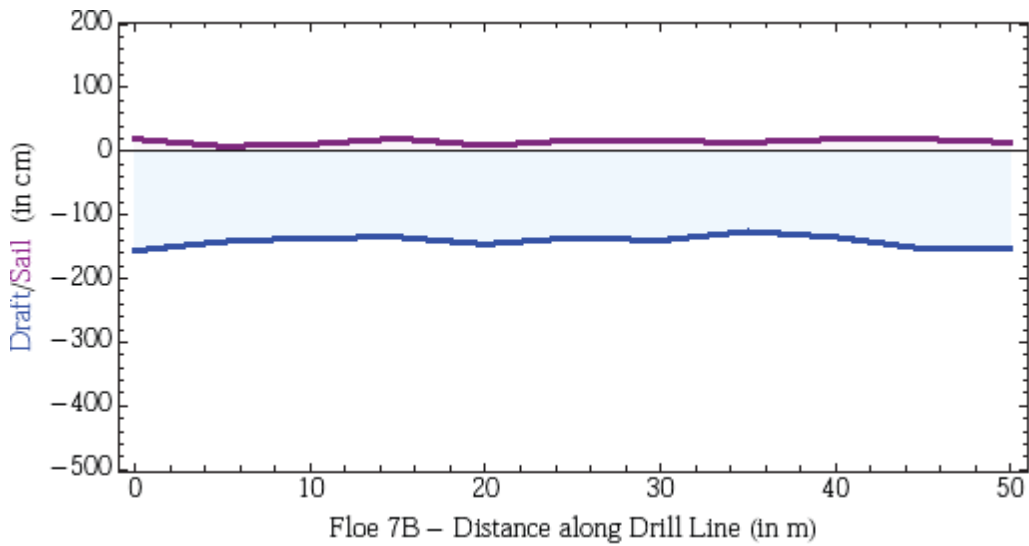
Floe 6 BLine



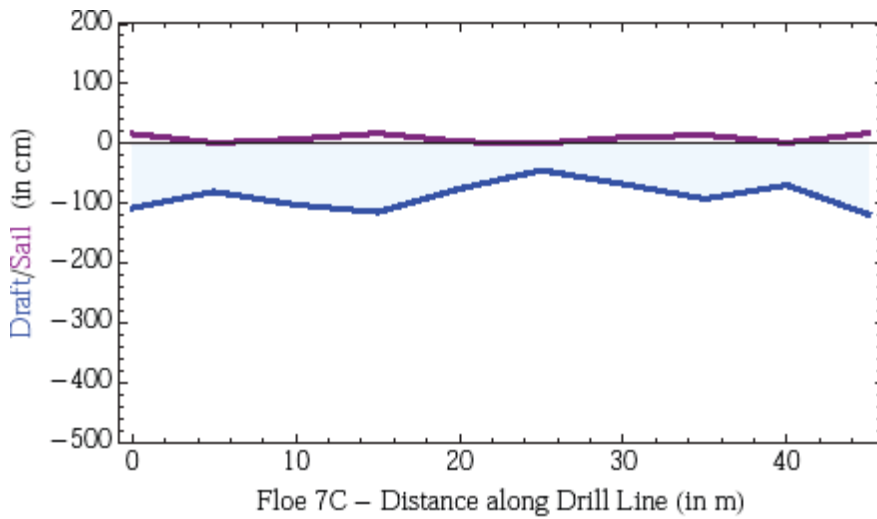
Floe 6 CLine



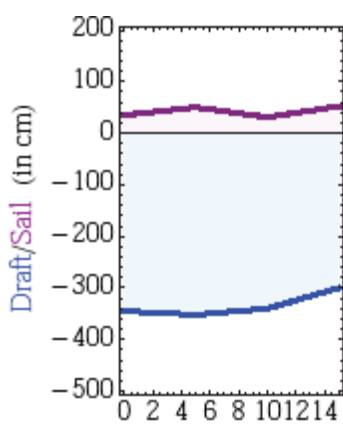
Floe 7A



Floe 7B

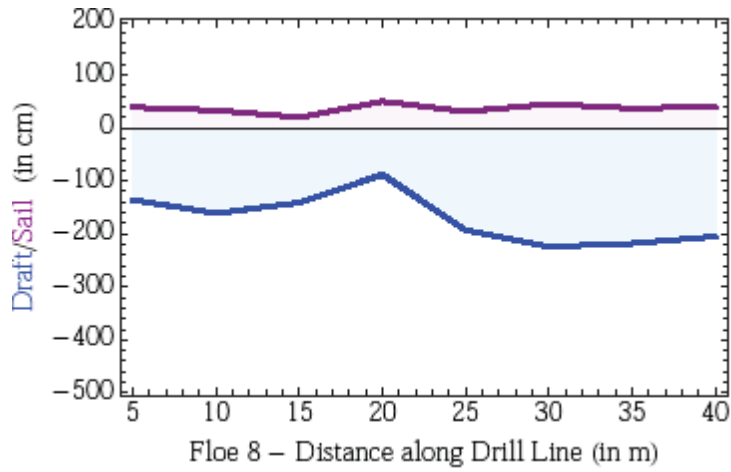


Floe 7C

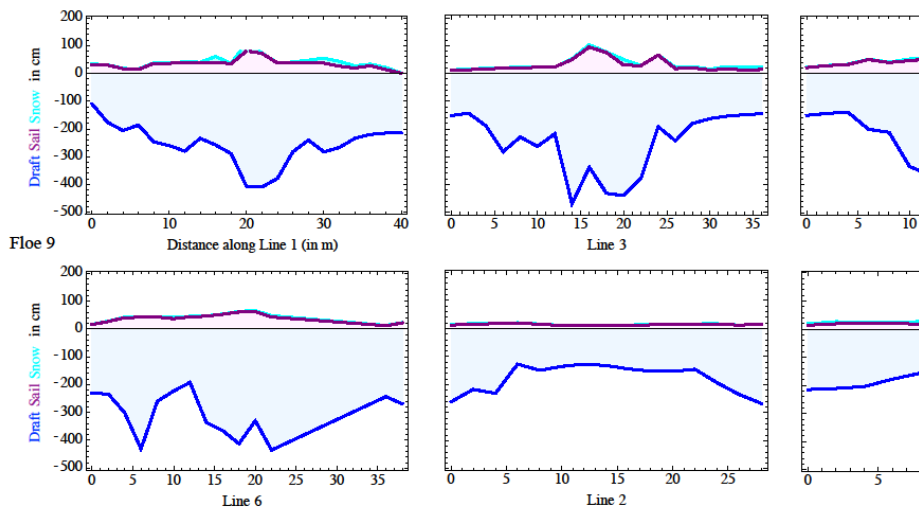


Floe 7D – Distance along Drill Line (in m)

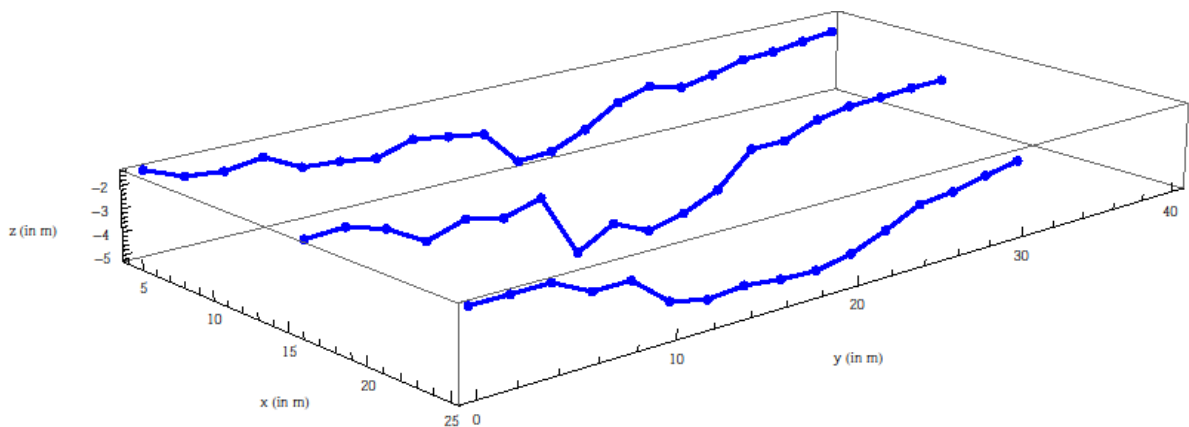
Floe 7D



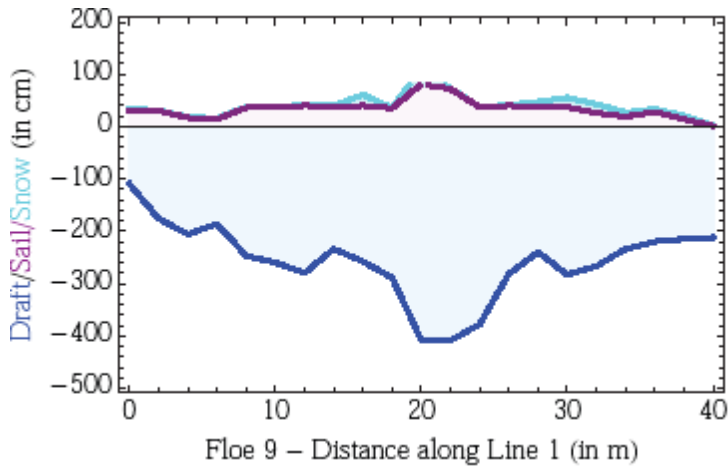
Floe 8



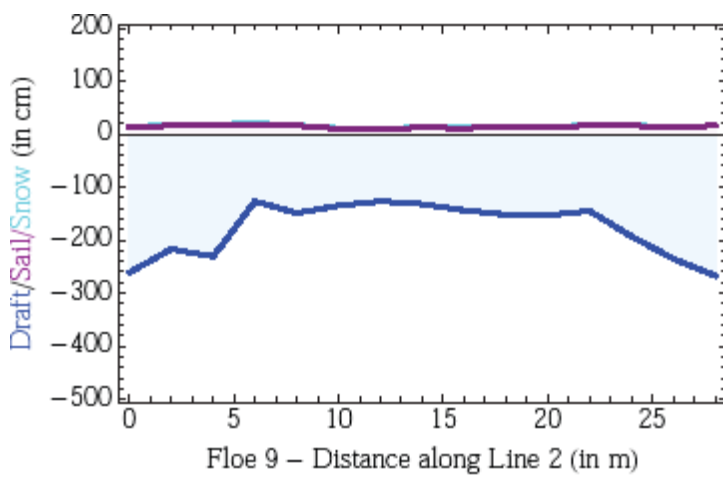
Floe 9 All Lines



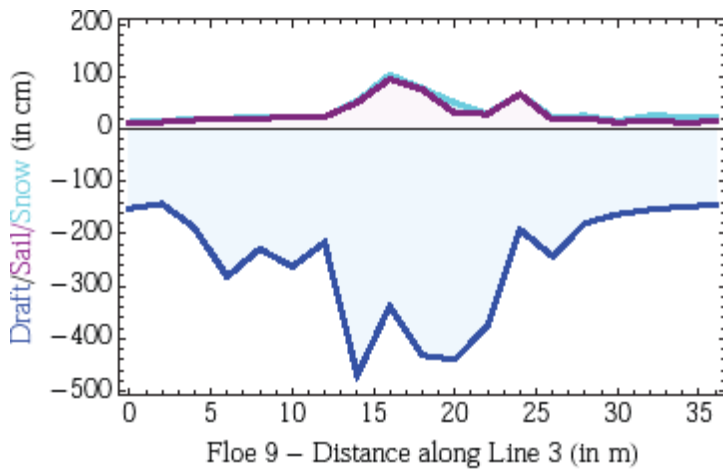
Floe 9 3D



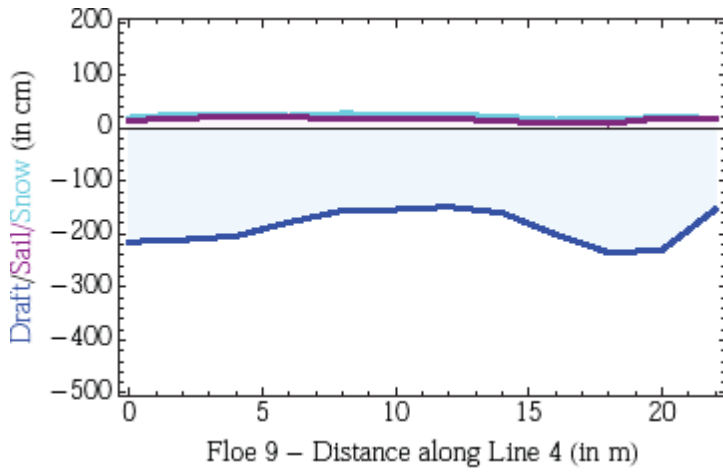
Floe 9 Line 1



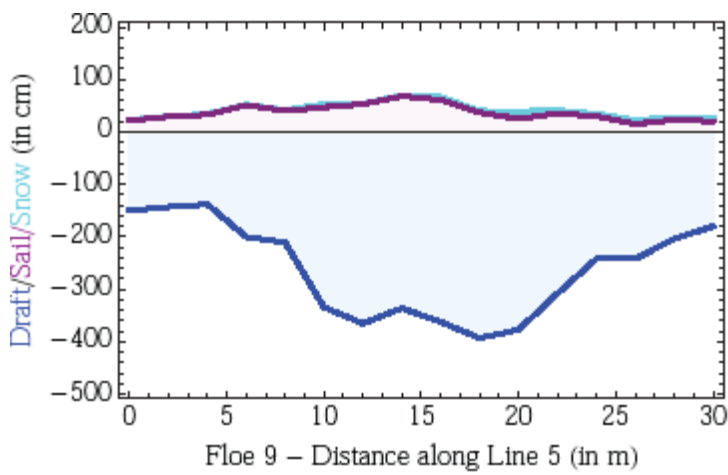
Floe 9 Line 2



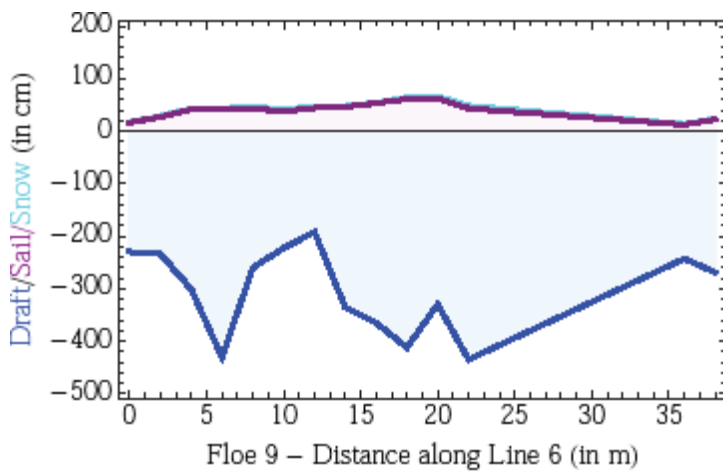
Floe 9 Line 3



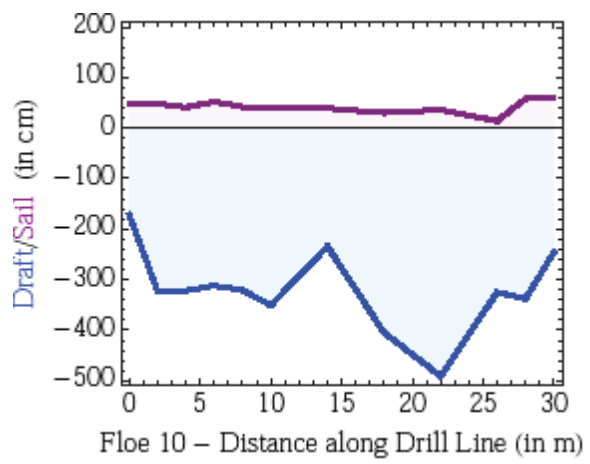
Floe 9 Line 4



Floe 9 Line 5



Floe 9 Line 6



Floe 10 ALine

**END OF DOCUMENT**